

Review

Correlative microscopy of Purkinje cells

ORLANDO J. CASTEJÓN*

Instituto de Investigaciones Biológicas “Drs. Orlando Castejón and Haydee Viloria de Castejón”. Facultad de Medicina. Universidad del Zulia. Maracaibo. Venezuela.

Key words: cerebellar cells, synaptic contacts, electron microscopy, immunohistochemistry.

ABSTRACT: The Purkinje cell and their synaptic contacts have been described using (1) light microscopy, (2) transmission and scanning electron microscopy, and freeze etching technique, (3) conventional and field emission scanning electron microscopy and cryofracture methods, (4) confocal laser scanning microscopy using intravital stain FM64, and (5) immunocytochemical techniques for Synapsin-I, PSD9-5, GluR1 subunit of AMPA receptors, N-cadherin, and CamKII alpha. The outer surface and inner content of plasma membrane, cell organelles, cytoskeleton, nucleus, dendritic and axonal processes have been exposed and analyzed in a three-dimensional view. The intramembrane morphology, in bi- and three-dimensional views, and immunocytochemical labeling of synaptic contacts with parallel and climbing fibers, basket and stellate cell axons have been characterized. Freeze etching technique, field emission scanning microscopy and cryofracture methods, and GluR1 immunohistochemistry showed the morphology and localization of postsynaptic receptors. Purkinje cell shows N-cadherin and CamKII alpha immunoreactivity. The correlative microscopy approach provides a deeper understanding of structure and function of the Purkinje cell, a new three-dimensional outer and inner vision, a more detailed study of afferent and intrinsic synaptic junctions, and of intracortical circuits.

Light microscopy and Golgi light microscopy

The Purkinje cells were first described at light microscopy (LM) level by Purkinje (1837), and subsequently by Denissenko (1877), Golgi (1882, 1886), Ramón y Cajal (1955a, b; 1890), Kölliker (1890), Retzius (1892), Dogiel (1896), Smirnov (1897), Held (1897), Crevatin (1898), Bielschowski and Wolff (1904), Lache (1906), Estable (1923), Jakob (1928), Fox and Barnard (1957), Fox (1962) and Fox *et al.* (1964).

Transmission electron microscopy

With the advent of transmission electron microscopy (TEM) Purkinje cells were meticulously examined in several vertebrates, mainly by Palay and Palade (1955), Gray (1961), Herndon (1963), Hamori and Szentágothai (1964, 1968), Eccles *et al.* (1967), Castejón (1968), Sotelo (1969), Mugnaini (1972) and Palay and Chan-Palay (1974). Gray (1961) first described by LM and TEM the Purkinje spine synapses. Herndon (1963) described by TEM the fine structure of Purkinje cells. Fox (1962), Fox *et al.* (1964, 1967), and Eccles *et al.* (1967) carried out Golgi LM and TEM studies of vertebrate Purkinje cells. The most detailed description of Purkinje cells by LM, TEM and Golgi

*Address correspondence to: Orlando J. Castejón.
E-mail: fundadesarrollo@iamnet.com
Revised version received: October 1, 2011. Accepted: October 15, 2011.

rapid impregnation by high voltage EM was given by Palay and Chan-Palay (1974). The recurrent collaterals of Purkinje cell axons were described by Chan-Palay (1971) and Chan-Palay and Palay (1971) by Golgi LM and TEM. Meek and Nieuwenhuys (1991) described, by means of a correlated LM and TEM study, the palisade pattern of Purkinje cell dendrites in Purkinje cells of a mormyrid fish. The smooth ER of Purkinje cell was analyzed in serial sections for TEM and semithin and thick sections for intermediate high voltage EM; it was seen forming a highly interconnected network of tubules and cisterns extended throughout the dendritic shaft and into the spines. García-Segura and Perrelet (1984) reported a postsynaptic membrane domain in the cerebellar molecular layer using the freeze-etching technique. Matsumura and Kohno (1991) observed, in serial sections for TEM and toluidine blue semithin sections for LM, the presence of microtubules fasciculated by cross-bridges in the perikaryon, axon hillock and initial axon segment of Purkinje cells. Alvarez-Otero *et al.* (1993) described the synaptic contacts in Purkinje cells of elasmobranch cerebellum. Castejón and Castejón (1997), using the freeze-fracture method for SEM applied to teleost fishes, showed at the longitudinal and cross sections of Purkinje secondary dendritic ramifications, the endoplasmic reticulum (ER) profiles and cytoskeletal elements forming a microtrabecular arrangement, in which mitochondria appear suspended. Kanaseki *et al.* (1998), using quick-freezing technique followed by freeze-substitution for ultrathin sectioning or freeze-fracturing and deep-etching replicas, showed that all smooth ER are rough-surfaces heavily studded with a large number of small dense projections. The localization of these projections coincides with the distribution of the inositol 1,4,5-triphosphate (IP3) receptor determined by quantitative immunogold electron microscopy.

Scanning electron microscopy

Castejón and Valero (1980) first described the human Purkinje cells at SEM level using the ethanol criofracturing technique designed by Humphreys *et al.* (1975). Castejón and Caraballo (1980a,b) described the SEM features of Purkinje cells in teleost fishes. Castejón and Castejón (1981) reported the TEM and SEM, and ultracytochemistry of Purkinje cells in vertebrate and human cerebellar cortex. Scheibel *et al.* (1981), by means of the creative tearing technique for SEM, exposed the outer surface of Purkinje cells, the surrounding basket cell axon collaterals and segments of climb-

ing fibers. Castejón (1983, 1988) described the scanning electron microscopic features of climbing fiber-Purkinje synapses, and parallel fiber-Purkinje spine synapses. Arnett and Low (1985) using ultrasonic microdissection showed at SEM level the Purkinje cells, the basket cell synapses and the Purkinje dendritic spines. Castejón (1990) carried out a freeze-fracture scanning electron microscopy and comparative freeze-etching study of parallel fiber-Purkinje spine synapses of vertebrate cerebellar cortex. Castejón and Apkarian (1992, 1993) reported a conventional and high resolution field emission scanning electron microscopy of outer and inner surface features of Purkinje cells, and their synaptic relationship with parallel fibers. Takahashi-Iwanaga (1992) showed the reticular endings of Purkinje cell axons in the rat cerebellar nuclei by means of sodium hydroxide maceration. Castejón *et al.* (1994) described the high resolution (SE-1) scanning electron microscopy features of Rhesus monkey cerebellar cortex. Hojo (1994) prepared specimens of human cerebellar cortex by means of tert-butyl alcohol freeze-drying device and examined the Purkinje cell somatic surface. Castejón and Castejón (1997) described in detail the three-dimensional morphology and synaptic connections of Purkinje cell of several vertebrates using conventional and high resolution scanning microscopy combined with the freeze-fracture method for SEM. Castejón and Sims (1999) described the Purkinje cells of hamster cerebellum using FM4-64 as an intracellular staining using confocal laser scanning microscopy. Castejón *et al.* (2001a) and Castejón (2003a) described in detail a correlative conventional and high resolution SEM, and an immunochemical study of vertebrate Purkinje cells.

Confocal microscopy

Castejón and Dailey (2009) using confocal laser scanning microscopy (CLSM) showed the synaptic relationship of Purkinje cells by means of immunohistochemistry study of synapsin-I and PSD-95. Confocal microscopy, using Dil as a fluorescent stain permitted to observe also a continuous compartment of ER from the cell body throughout the dendrites (Terasaki *et al.*, 1994). By means of CLSM, using FM4-64 as an intravital stain, the Purkinje cell body, primary trunk, secondary and tertiary spiny dendritic ramifications were clearly visualized, and the climbing fibers, basket cell and stellate cell axons were observed approaching to the Purkinje cell soma (Castejón and Sims, 1999, 2000; Castejón *et al.*, 2001a).

Immunoelectron microscopy

The distributions of taurine-like and GABA-like immunoreactivities in the rat cerebellum were compared by analysis of consecutive semithin and ultrathin sections, postembedding labeled with the peroxidase-antiperoxidase technique or with an indirect immunogold procedure, respectively (Ottersen *et al.*, 1988a). Taurine-like immunoreactivity was selectively enriched in Purkinje cell bodies, dendrites and spines (Ottersen *et al.*, 1988b).

Ige *et al.* (2000) showed by double immunofluorescence technique and TEM, the localization of GABA (B1) and GABA (B2) receptor subunits in the membranes of Purkinje cell dendritic spines and in parallel fibers. Mateos *et al.* (1998) showed by LM and post-embedding immunogold method for TEM, the subcellular localization of mGlu4a metabotropic glutamate receptor in parallel fiber-Purkinje spine synapses. Other histochemical and ultrastructural investigations, have demonstrated the existence of a heterogeneous population of Purkinje cells (Monteiro *et al.*, 1994).

The subcellular distribution of endoplasmic reticulum proteins (IP3R1 and RYR), plasma membrane (PM) proteins (mGluR1 and PMCA Ca(2+)-pump), and scaffolding proteins, such as Homer 1b/c, was assessed by laser scanning confocal microscopy of rat cerebellum parasagittal sections (Sandona *et al.*, 2003). Ca(2+) stores may contribute to spontaneous GABA release onto mouse Purkinje cells (Bardo *et al.*, 2002).

Dark and clear Purkinje cells

Tewari and Bourne (1963) published a histochemical study of dark and light Purkinje cells. Castejón and Castejón (1972, 1976, 1981) reported the presence of dark and clear Purkinje cells in mouse cerebellar cortex using osmium-DMEDA as the primary fixative, followed by glutraldehyde-Alcian blue mixture. Both cell types exhibited the presence of acid glycosaminoglycans or proteoglycans at electron microscopy level (Figs.1 and 2).

Bosel'ová *et al.* (1978) described the Golgi apparatus of clear and dark Purkinje cells. Avruschenko and Marshak (1983) distinguished clear and dark Purkinje cells during the post-resuscitation period. The authors suggested that light and dark PC differ in their roles in the maintenance of the population homeostasis rather than in the metabolic rate. Khan (1993) by means of histochemical and ultrastructural investigations also demonstrated the existence of a heterogeneous popula-

tion of Purkinje cells. Monteiro *et al.* (1994) related the presence of these two populations of Purkinje cells with the morphological changes that take place with ageing and nerve cell death. More recently, conventional electron microscopy of human cerebellar cortex has also revealed two types of Purkinje neurons with different staining intensities. The light-stained type constitutes the major type, and both types have similar diameters (El Dwairi, 2007). The existence of these two populations of Purkinje cells deserve further investigations, mainly the relationship of dark Purkinje cells with ischemic-anoxic processes and nerve cell death. The possibility of artifact fixation should also be explored. A further study with confocal scanning microscopy using specific labeling should also be performed.

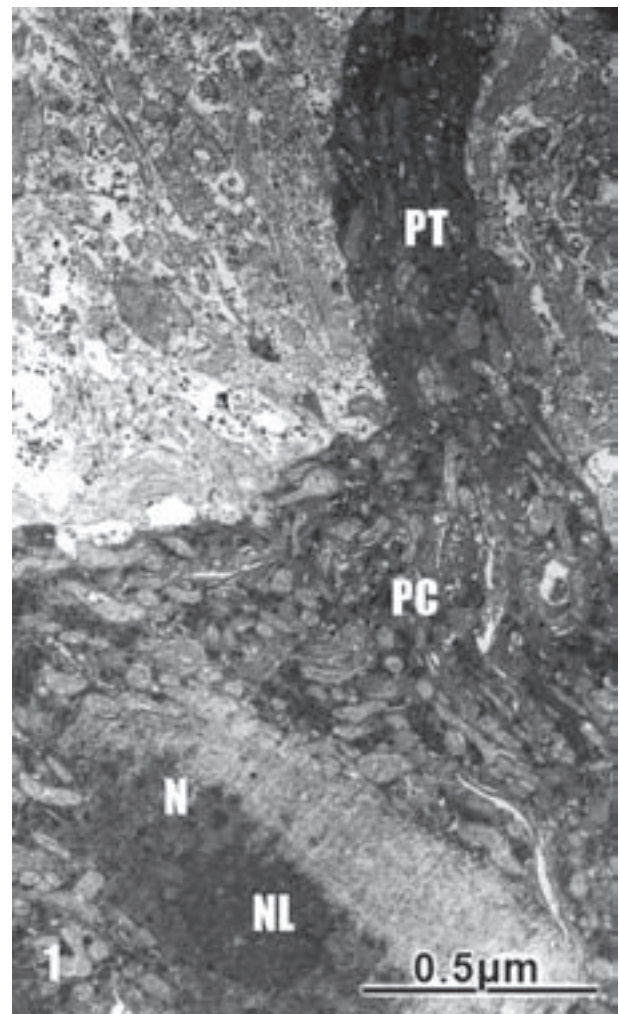


FIGURE 1. Mouse cerebellar cortex. Dark Purkinje cell (PC) fixed with a glutaraldehyde-Alcian Blue mixture and displaying a notably stained nucleolus and perinucleolar chromatin, and a less stained nuclear (N) clear peripheral chromatin. The cytoplasmic matrix exhibits dark alcianophilic patches suggesting the presence of proteoglycan macromolecules surrounding the free ribosomes.

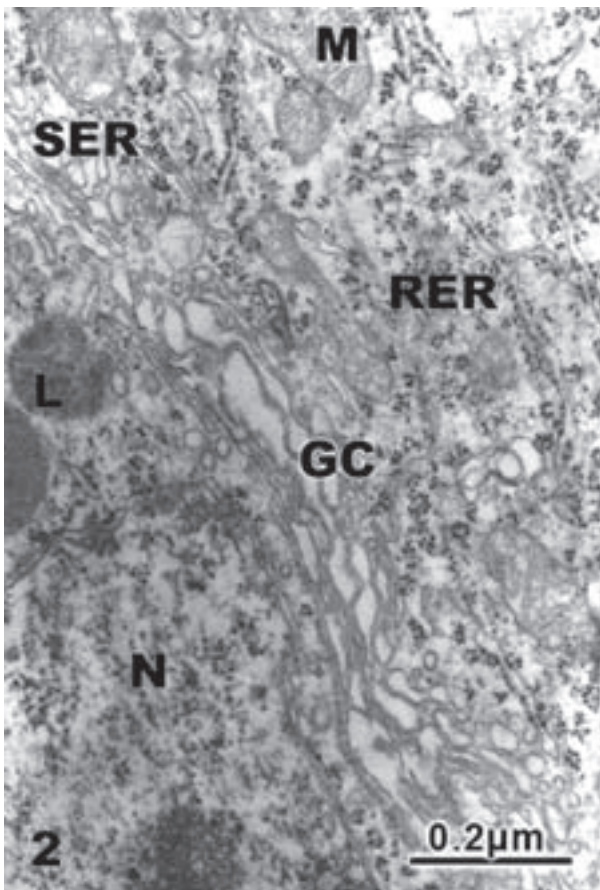


FIGURE 2. Mouse cerebellar cortex. Gluraldehyde-osmium fixation. Clear Purkinje cell showing the rough (RER) and smooth (SER) endoplasmic reticulum, a large Golgi complex (GC), mitochondria, and a clear nuclear (N) chromatin.

Purkinje cell rough surface endoplasmic reticulum

Purkinje cells exhibit as a well developed rough ER, similar to that observed in liver, salivary and plasma cells, which is related with its great protein biosynthetic machinery. The rough ER comprises a regular array of flat cisterns surrounded by literally clouds of either attached and free polyribosomes, interconnected with branching tubules and sacs extended throughout the cytoplasm. (Palay and Palade, 1955; Herndon, 1963; Fox *et al.*, 1964; Castejón, 1968; Palay and Chan-Palay, 1974; Kiiashchenko and Severina, 1993; Rusakov *et al.*, 1993). (Fig. 2).

Immunofluorescence and immunogold labeling, together with sucrose gradient separation and Western blot analysis of microsomal subfractions, were employed in parallel to probe the ER in the cell body and dendrites of rat cerebellar Purkinje neurons. Two markers,

previously investigated in non-nerve cells, the membrane protein p91 (calnexin) and the luminal protein BiP, were found to be highly expressed and widely distributed to the various endoplasmic reticulum sections of Purkinje neurons, from the cell body to dendrites and dendritic spines (Villa *et al.*, 1992). Antibodies to protein kinase C delta produced a very different labeling pattern in the Purkinje cells. Most of the gold particles are associated with the rough ER, particularly with those cisternae that are located close to the nucleus or in the nuclear indentations (Cardell *et al.*, 2003).

Transcripts for P2Y2 receptors, marked by the gold-silver grains, were revealed in Purkinje cells (Loesch and Glass, 2006). Transcripts are essentially localized in the cytoplasm although they also appeared to be specifically associated with granular ER. This finding suggests that Purkinje cells may produce functional P2Y2 receptors involved in the ATP-related regulatory role in the cerebellum (Loesch and Glass, 2006).

Smooth endoplasmic reticulum

The smooth ER also is quite prominent in Purkinje cell cytoplasm. Specialized arrangements termed annulate lamellae and subsurface system can also distinguished (Fig.2). Secondary lysosomes or phagosomes, and lipofuscin granules are dispersed throughout the cytoplasm. Mitochondria, microtubules and neurofilaments can be appreciated within the soma and the dendritic arborization, as well as in the axon and its recurrent collaterals.

Ross *et al.* (1989) first demonstrated in cerebellar Purkinje cells the localization of InsP3 receptor in rough ER, a population of smooth-membrane-bound organelles, a portion of subplasmalemmal cisternae and the nuclear membrane, but not in mitochondria or the cell membrane. InsP3 induces intracellular calcium mobilization. In Purkinje cell bodies, both the InsP3 and ryanodine receptors are present in smooth and rough ER, subsurface membrane cisternae, and to a lesser extent in the nuclear envelope (Walton *et al.*, 1991). An endoplasmic reticulum Ca²⁺ ATPase present in Purkinje cell endoplasmic reticulum (termed SERCA-2) appears to be involved in Ca²⁺ uptake into ER for release by inositol 1,4,5-trisphosphate, and other agents (Miller *et al.*, 1991).

The size and number of stacks of smooth ER are variable depending on their intracellular localization; short stacks with 2-4 parallel cisterns predominate in the perikaryon, while long stacks with 4-15 cisterns predominate in proximal dendrites and long stacks with

3-4 cisterns predominate in distal dendrites (Yamamoto *et al.*, 1991). Buchanan *et al.* (1993) postulated that the major calcium storage organelle in Purkinje cell dendrites is the ER, of which there are two types that can be distinguished by their calcium levels.

The three-dimensional organization of the smooth ER in Purkinje cell dendrites in the chick cerebellum form a highly interconnected network of tubules and cisterns extending throughout the dendritic shaft, and into the spines. Several distinct morphological domains of ER are noted, including the hypolemmal cisternae, the endomembranes associated with the dendritic spines, and the tubular and cisternal endoplasmic reticulum in the dendritic shaft (Martone *et al.*, 1993). According to these authors the ER forms a complicated network that may be part of a single endomembrane system within Purkinje cells. Stacks of regularly spaced, flat, smooth-surfaced endoplasmic reticulum cisternae frequently observed in both the cell body and dendrites of cerebellar Purkinje neurons, and are immunocytochemically shown to be highly enriched in receptors for the second messenger, inositol 1,4,5-trisphosphate (Rusakov *et al.*, 1993).

The *in vivo* structure of the smooth ER was visualized in rat and mouse cerebellar Purkinje cells by using quick-freezing techniques followed by freeze-substitution for ultrathin-sectioning or freeze-fracturing and deep-etching for replicas. High magnification electron microscopy of the ultrathin sections revealed the surprising finding that all the smooth ER are apparently rough surfaced, and heavily studded with a large number of small dense projections. In the soma the smooth ER appears to be similar to its rough counterpart. The localization of the projections coincides with the intracellular distribution of the inositol 1,4,5-trisphosphate (IP₃) receptor determined by quantitative immunogold electron microscopy. These findings would suggest that the projections are tetramers of IP₃ receptor molecules and could be used as a morphological marker for the smooth ER in Purkinje cells (Kanaseki *et al.*, 1998).

An excess release of excitatory transmitter by brief anoxia activates metabotropic glutamate receptors, which transform the smooth ER networks into lamellar bodies, that normally release Ca²⁺ widely to the neuronal cytoplasm. Large Ca²⁺ storage pools of lamellar bodies are formed by the association of opposing molecules that belong to different cisternae and may protect from excess release of Ca²⁺ from their reservoirs (Banno and Kohno, 1998).

The Golgi apparatus of Purkinje cell

In the late 1890's, 25 years after the publication of his black reaction Camilo Golgi noticed a fine internal network in only partially silver-osmium-blackened Purkinje cells. Following confirmation by his assistant Emilio Veratti, Golgi published the discovery, called the "apparato reticolare interno", in the *Bollettino della Società Medico-chirurgica di Pavia* in 1898, which is now considered the birthday of the "Golgi apparatus" (Dröscher, 1998). The Golgi apparatus is highly specialized, and consists of aggregates of smooth-walled cisterns surrounded by a large variety of vesicles, such as simple vesicles and coated or alveolate vesicles (Fig.2). It is surrounded by a heterogeneous assemblage of organelles, including mitochondria, lysosomes, and multivesicular bodies. The Golgi apparatus is observed in the perinuclear region, but is also found throughout the cytoplasm and extends into dendrites. Primary lysosomes are also seen emerging from the Golgi saccules.

No cell excels Purkinje neurons in beauty of the Golgi apparatus, whether demonstrated by classical techniques or by nucleoside diphosphatase or thiamine pyrophosphatase activity (Novikoff, 1967). Novikoff postulated the GERL complex to designate the interrelated system formed by Golgi apparatus, endoplasmic reticulum, and lysosomes. Radioautographic and ultracytochemistry evidences demonstrate that concentration of complex polysaccharide occur in the Golgi apparatus (Peterson and Leblond, 1964; Castejón and Castejón, 1972). The Golgi apparatus acquires newly synthesized proteins from ER in which undergo a variety of posttranslational modification, including glycosylation, sulfation, and proteolytic cleavage and packaging, as well as for sorting. The proteins and glycoproteins are then transferred to simple and coated vesicles that bud off the trans-Golgi membranes, and move to the cell surface and processes of the Purkinje neuron, resulting in the incorporation of vesicle membrane proteins into the plasma membrane (exocytosis). This form of secretion has been termed constitutive secretion. Sorting of newly synthesized proteins occurs in the Golgi apparatus. Passage through the Golgi apparatus is obligatory for most proteins destined for fast axonal transport. Transfer from the Golgi complex to the fast axonal transport appears to be mediated by clathrin-coated vesicles (Castejón, 2008).

Gao *et al.* (2009) have recently reported that four members of the zinc transporter (ZNT) family, ZNT1, ZNT3, ZNT4, and ZNT6, are abundantly expressed in

the Golgi apparatus of Purkinje cell suggesting suggest a significant role of ZNT7 in zinc homeostasis in the mouse cerebellum.

According to Mashimo *et al.* (2008) in cultured Purkinje cells, stimulation of AMPA receptors, but not metabotropic glutamate receptors, triggered translocation of cPLA(2)alpha to the somatic and dendritic Golgi compartments. Cytosolic phospholipase A(2)alpha (cPLA(2)alpha) selectively releases arachidonic acid from membrane phospholipids, and has been proposed to be involved in the induction of long-term depression (LTD), a form of synaptic plasticity in the cerebellum.

Members of the Rab subfamily of small GTPases play an important role in the regulation of intracellular transport routes. Rab6A has been shown to be a regulator of membrane traffic from the Golgi apparatus towards the ER. Rab6B was found to be specifically expressed in microglia, pericytes and Purkinje cells themselves (Opdam *et al.*, 2000).

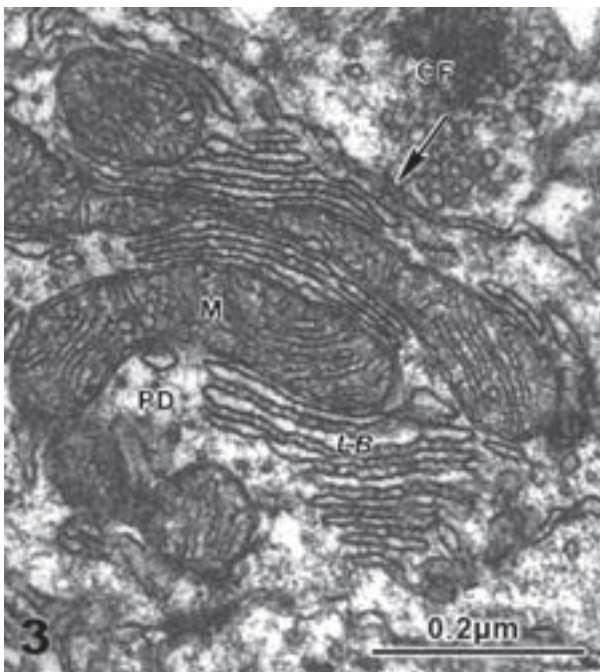


FIGURE 3. Mouse cerebellar cortex. Purkinje cell dendrite (PD) showing the intimate relationship between slender mitochondria (M) and annulate lamellae or lamellar bodies (LB). The arrow labels a climbing fiber- Purkinje axodendritic synapse.

Lysosomes

Lysosomes, dense bodies and lipofuscin granules are observed in the cytoplasm of Purkinje cells (Fig. 2). Lysosomes and pigment granules were earlier described by Shinonaga in Purkinje cells (1962). Immunoelectron microscopic localization of cathepsin D in Purkinje cells was investigated using protein A-gold technique. Gold particles representing the antigen sites of cathepsin D were localized in lysosomes of Purkinje cells (Yakota and Atsumi, 1983). The genesis, structure and transit of dense bodies in rat neocerebellar cortical Purkinje neurons were earlier studied by Monteiro (1991).

Mitochondria

Clear and dark mitochondria are observed in Purkinje cells. Some Purkinje cell mitochondria exhibit topographic relationship with annulate lamellae. Slender mitochondria are observed mainly in Purkinje cell dendritic processes (Fig. 3).

The ultrastructural demonstration of succinate semialdehyde dehydrogenase (SSADH) activity in cerebellar Purkinje neurons was demonstrated by Bernocchi *et al.* (1986). SSADH activity was localized on the mitochondria especially on the outer membrane; some extra mitochondrial formazan deposits were also found. The activities of the enzymes cytochrome oxidase (COX) and succinic dehydrogenase (SDH) were evidenced by means of the diaminobenzidine and copper ferrocyanide preferential cytochemical techniques, respectively. At the electron microscope, the activities of these two key molecules of the respiratory chain were clearly visualized as dark precipitates at the inner mitochondrial membrane sites (Bertoni-Freddari *et al.*, 2001). The monoclonal antibody M-II 68 recognizes Purkinje cell inner mitochondrial membrane in routinely processed formalin-fixed and paraffin-embedded tissue by light microscopy immunohistochemistry (Paulus *et al.*, 1990).

The cytoskeleton of Purkinje cell

Cytoskeletal structures such as microtubules, neurofilaments, and microfilaments are observed in the cell body, dendrites and axon (Fig. 4).

The distribution of microtubule-associated protein 1A (MAP1A) in Purkinje cells was studied by Shiomura and Hirokawa (1987) by means of electronmicroscopic immunocytochemistry, using a monoclonal antibody (McAb) against MAP1A; this was combined with the observation of the three-dimensional cytoskeletal ultra-

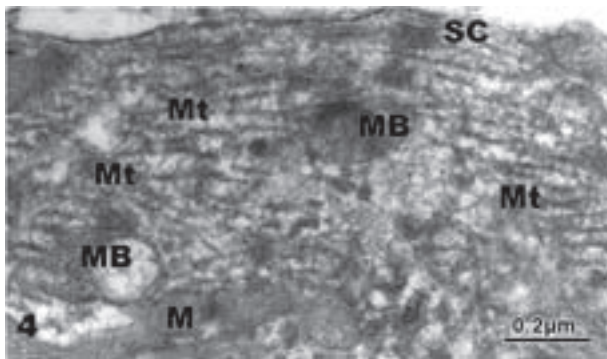


FIGURE 4. Mouse cerebellar cortex. Vascular perfusion with gluraldehyde-Alcian blue mixture. Purkinje cell secondary dendrite showing bundles of dense microtubules (Mt) with lateral projections joining adjacent microtubules. Mitochondria (M), sublemmal canaliculi (SC), and multivesicular bodies (MB) also are seen. A sublemmal coating (SC) is observed due to Alcian blue-OSMEDA ultracytochemical satining staining (Castejón and Castejón, 1972).

structure in dendrites via the quick-freeze, deep-etch technique (QF-DE). The three-dimensional cytoskeletal ultrastructure of fresh Purkinje cell dendrites was revealed by QF-DE. In Purkinje cell dendrites, microtubule was a predominant cytoskeletal element, whereas only a few neurofilaments are found. Fine, elaborate cross-bridges filled up the interstices among and between microtubules and other cellular components. Cross-bridges linking microtubules to one another are mainly composed of a fine filamentous structure, with frequent branching and anastomosing at several sites, and appearing somewhat granular.

According to Meller (1987), the cytoskeleton of Purkinje cells (PC) shows distinct domains and composition of filamentous structures in the different cytoplasmic regions (perikaryon, dendritic cytoplasm and axoplasm). The perikaryon is occupied by a meshwork of fine filaments, 4-7 nm in diameter, which extends from the nuclear outer membrane to the cell membrane. In this zone, the cell organelles (e.g., endoplasmic reticulum, mitochondria) adopt a circular arrangement around the nucleus. All structures are anchored by microfilaments to the cytoplasmic network. The dendrites show a dense cytoplasmic network including bundles of microtubules, neurofilaments and microfilaments. Numerous aggregated globular components are attached to this cytoskeleton. The cytoskeleton of the dendritic spines shows axially oriented 10-nm bundles of filaments, which are interconnected and also anchored by cross-

linkers to the cell membrane and to components of the agranular endoplasmic reticulum.

Purkinje cell dendrites

With the Golgi light microscopy technique the elaborated dendritic ramification of Purkinje cell can be seen extended throughout the cerebellar molecular layer (Fig. 5). The Purkinje primary dendritic trunk, secondary and tertiary dendrites can be easily distinguished.

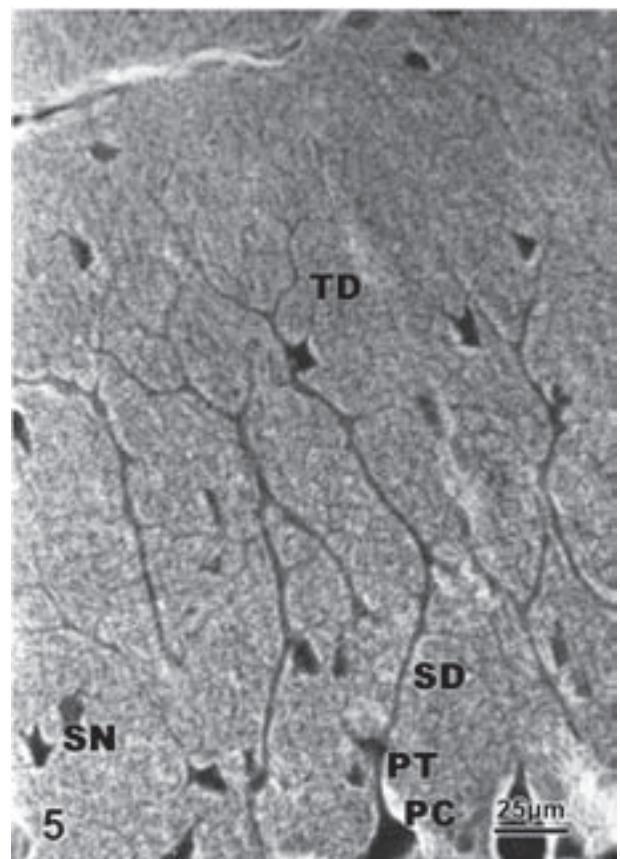


FIGURE 5. Mouse cerebellar cortex. Golgi light microscopy. A Purkinje cell (PC) shows the primary dendritic trunk (PT), the secondary (SD) and tertiary (TD) dendrites.

Transmission electron microscopy shows that structural elements in the Purkinje cell body extend through the primary dendritic processes, and to secondary and tertiary dendrites. The primary dendritic trunk shows axospino- and shaft axodendritic contacts with climbing fiber endings (Castejón, 1983; Castejón and Sims, 2000), and appears surrounded at certain inter-

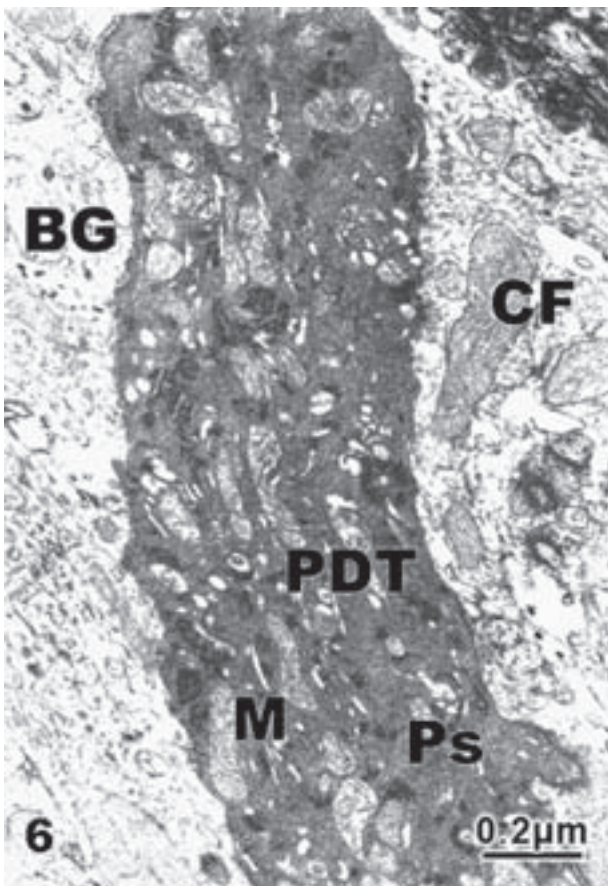


FIGURE 6. Dark Purkinje cell primary dendritic trunk (PDT) fixed with glutaraldehyde-Alcian blue mixture showing slender mitochondria (M), and a short dendritic spine (Ps) synapsing with a climbing fiber ending. The dark patches at the dendroplasm correspond to ribosome accumulations. The clear Bergmann glial cell cytoplasm (BG) appears ensheathing the primary dendritic trunk. Also note the axodendritic shaft synapse with a large climbing fiber ending (CF).

vals with Bergmann glial cell cytoplasm (Castejón, 2011). (Fig. 6).

The presence of annulate lamellae or lamellar bodies in Purkinje cell dendrites allows to characterize these structures at the molecular layer, and to differentiate them from Golgi, stellate and basket cell dendrites (Figs. 3 and 7).

The freeze-fracture method for scanning electron microscopy allowed us to disclose the three-dimensional view of mouse Purkinje cell secondary dendrite inner structure (Figs. 8 and 9) showing the three-dimensional appearance of anastomotic cisterns of endoplasmic reticulum, and mitochondria (Castejón, 1988).

By means of freeze-etching technique for transmission electron microscopy the intramembrane morphology of Purkinje cell dendritic membrane and the spine dendritic membrane is disclosed in figure 10, showing at the P face the homogeneous distribution of intramembrane particles (IMPs). (Castejón *et al.*, 2001b).

The fracture face and the E face of Purkinje cell tertiary dendritic membrane are characterized by their smooth fractured cytoplasmic surface and the pits left by transmembrane proteins detached during the freeze-etching procedure. (Castejón, 2010). (Figs. 11 and 12).

Novel laser-scanning modes for two-photon microscopy enable *in vivo* imaging of spatiotemporal activity patterns in Purkinje cell dendrites (Göbel and Helmchen, 2007) revealing fast dendritic calcium dynamics, and facilitating optical probing of dendritic function *in vivo*.

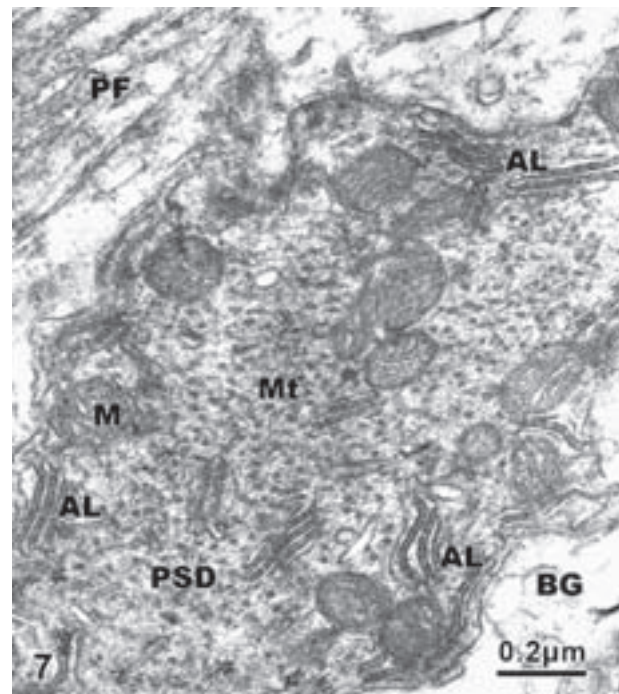


FIGURE 7. Mouse cerebellar cortex. Purkinje cell secondary dendrite (PSD) showing annulate lamellae (AL), mitochondria (M), and microtubules (Mt). Note the intimate apposition of Bergmann glial cell (BG) cytoplasm to Purkinje dendritic limiting membrane. The neighboring parallel fibers (PF) also are seen.

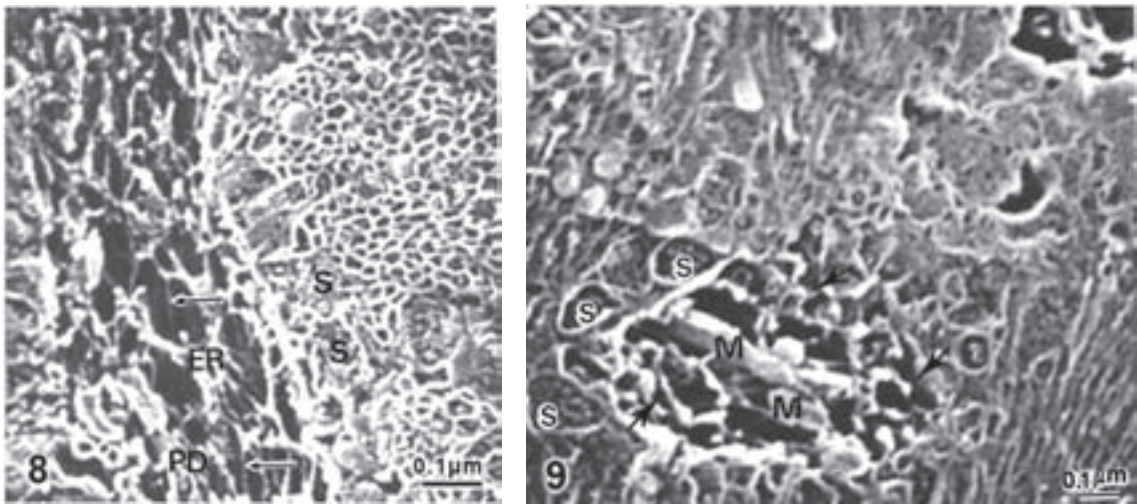


FIGURE 8. Scanning electron microscopy and cryofracture method. Longitudinal section of a Purkinje cell secondary dendrite (PD) displaying the interconnected system formed by endoplasmic reticulum cisternae (ER). The microtubules also are noted (arrow). The neighboring parallel fiber synaptic endings (S), and the non-synaptic segment of parallel fibers and slender mitochondria (M) also are distinguished. (Castejón, 1990a).

FIGURE 9. Scanning electron microscopy and cryofracture method. Cross section of a fractured Purkinje cell secondary dendrite showing the canaliculi of endoplasmic reticulum (arrows), and the outer surface of slender mitochondria (M). Note the cross sections of surrounding synaptic endings (S). (Castejón, 1990a).

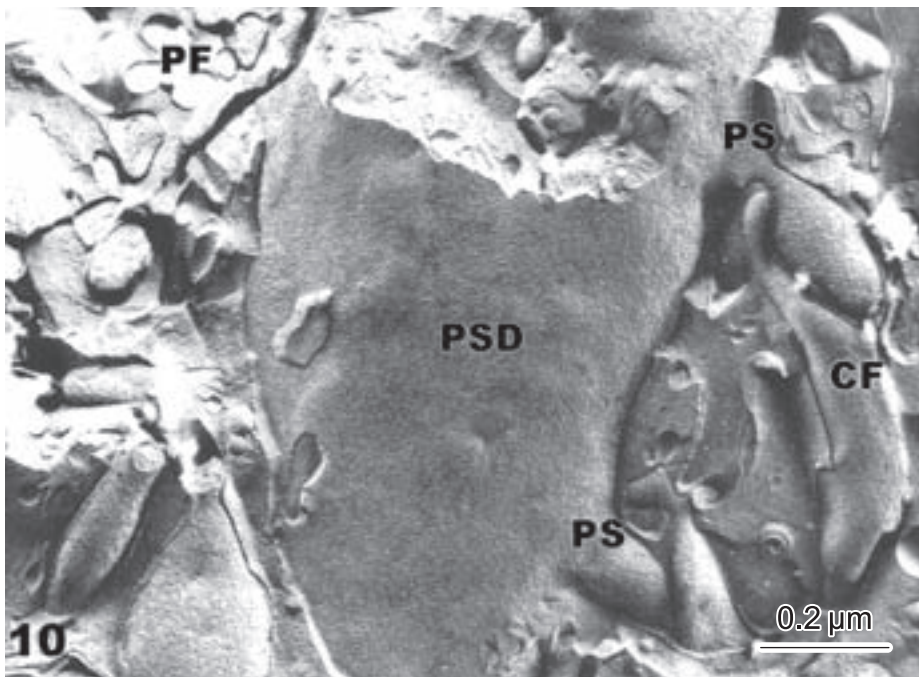


FIGURE 10. Secondary dendrite of a mouse Purkinje cell and their spines (PS) showing the homogeneous distribution of intramembrane particles at the plasma membrane P face (PfPd). Note the climbing fiber ending (CF) making synaptic contact with the spine neck. The cross sections of parallel fibers (PF) also are seen at the upper left angle of the figure. (Castejón, 1990b).

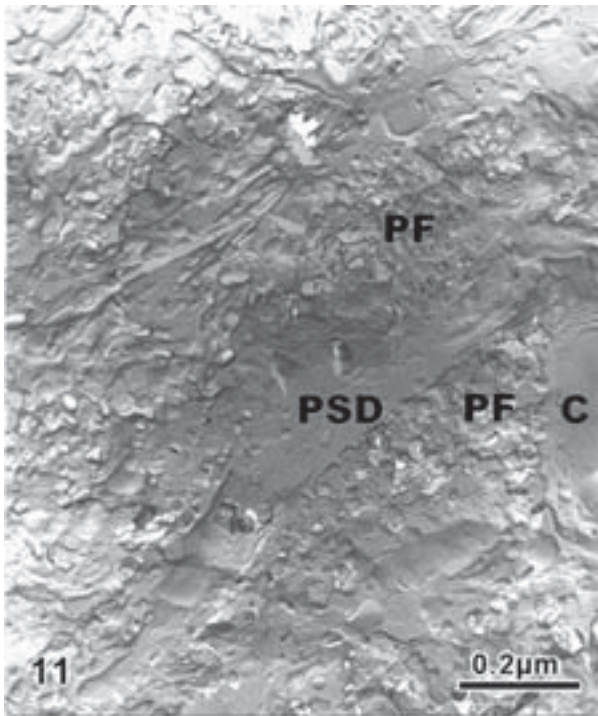


FIGURE 11. Mouse cerebellar molecular layer. Fracture face of a Purkinje secondary dendrite (PSD) surrounded by the cross fracture sections of parallel fibers (PF). A capillary (C) also is seen. (Castejón, 2010).

Purkinje cell axon

The axon of Purkinje cell emerges from the basal pole of the cell body. Calbindin and Cy5 labeling of rat cerebellar cortex (Castejón and Dailey, 2009) shows the course of Purkinje cell axons, and their collateral descending through the granular layer (Fig. 13).

The outer surface of Purkinje cell soma and the axonal initial segment can be appreciated with conventional scanning electron microscopy. (Castejón and Caraballo, 1980a,b). (Figs. 14 and 15).

Confocal laser scanning microscopy using Methamorph image analysis software allowed us to characterize the Purkinje cell axonal initial segment in z-series of hamster cerebellar cortex (Castejón and Sims, 1999). (Fig. 16).

At transmission electron microscopy the Purkinje cell axon hillock region or initial axonal segment appears unmyelinated and its axolemma displays a characteristically granular electron-dense undercoating (Chan-Palay, 1971). Basket cell axons cover most of its surface area with axo-axonic synapses (Mugnaini, 1972; Palay and Chan-Palay, 1974).

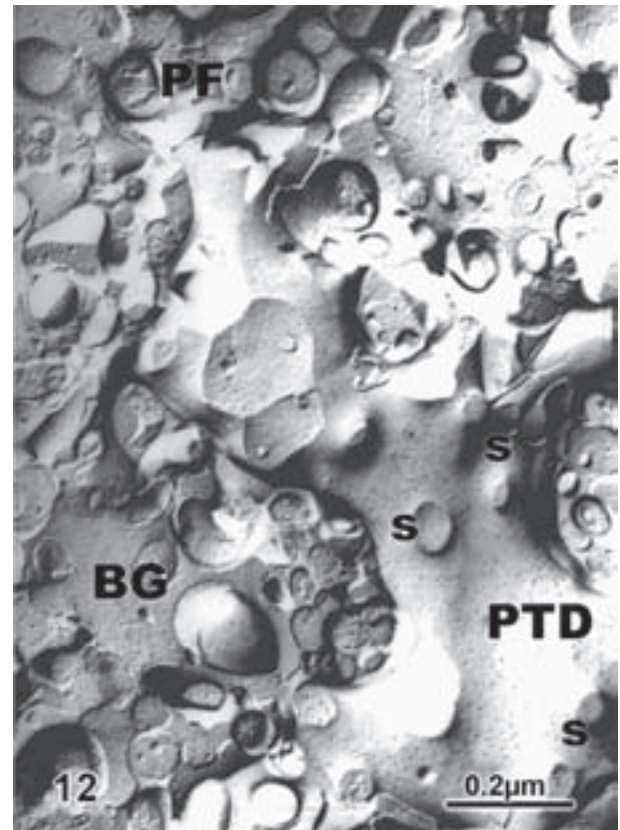


FIGURE 12. E face of tertiary dendrite of a mouse Purkinje cell (PTD) showing the pits left by detached intramembrane particles during the freeze-etching procedure. Note the cross sections of the spine necks (S), the neighboring Bergmann glial cell cytoplasm (BG), and the cross sections of parallel fibers (PF). (Castejón, 2010).

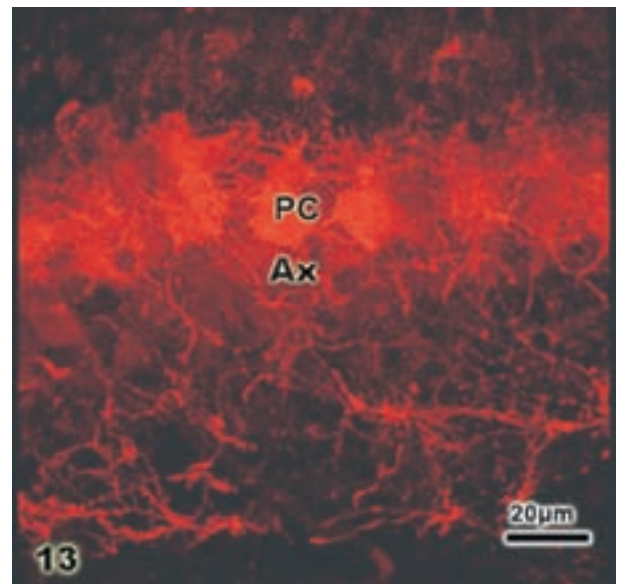
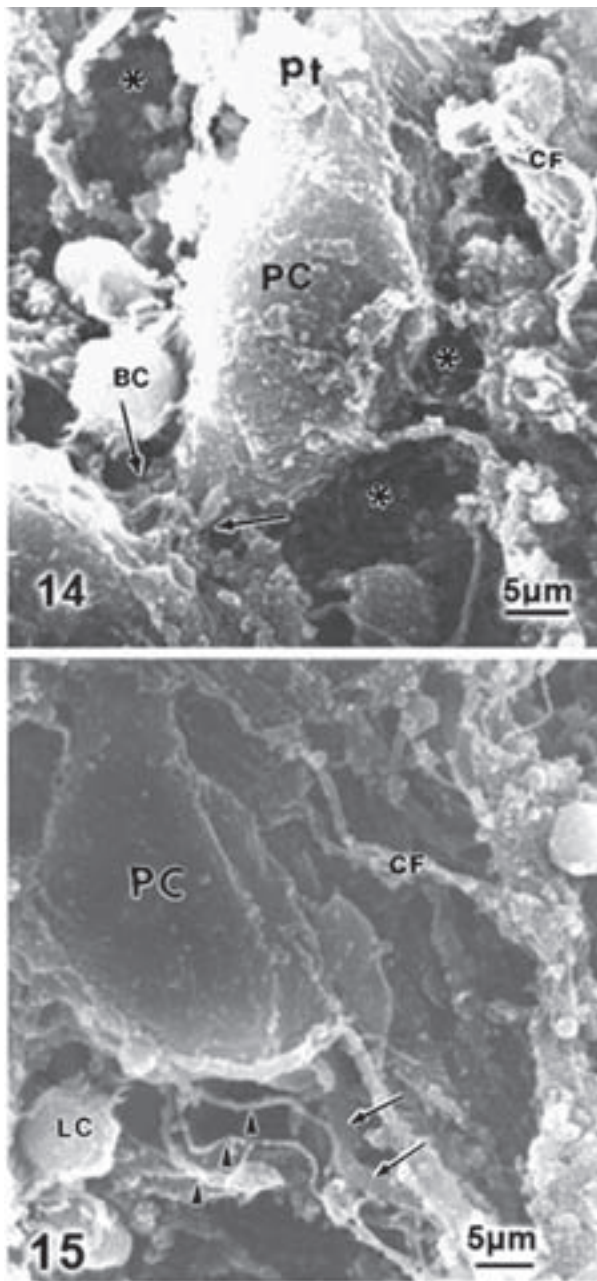


FIGURE 13. Rat cerebellar slice labeled with calbindin and Cy5 showing the red staining of Purkinje cell bodies and their axon directed toward the granular layer. Note the distribution of axonal recurrent collaterals in the granular layer. (Castejón, 2010).



Purkinje cell myelinated axons can be observed in their course through the granular layer and cerebellar white matter (Fig. 17).

As shown above (Fig. 13), the Purkinje cell axons give rise to several recurrent collaterals while passing through the granular layer (Castejón and Castejón, 1991; Castejón *et al.*, 2000a). These collaterals ascend to the Purkinje cell layer and can be seen at the molecular layer as myelinated axons surrounded by parallel fibers and Bergmann glial cell cytoplasm. (Castejón, 2010). Purkinje cell axon terminal endings exhibit a flat type of synaptic vesicles, which support their inhibitory na-

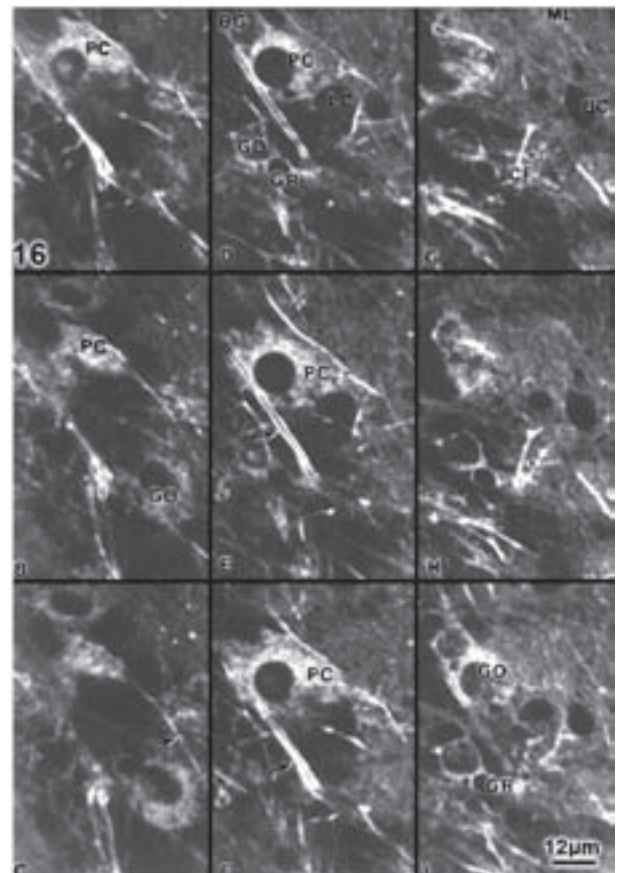


FIGURE 14. Sagittally cryofractured cerebellar cortex of a teleost fish showing the outer surface of Purkinje cell (PC) soma. The cryofracture method has removed the ensheathing Bergmann glial cell cytoplasm exposing the outer surface of the pear-shape neuronal soma. Note the emergency of primary dendritic trunk (pt). Climbing fibers (CF) are seen approaching the primary dendritic trunk. The asterisks label the dark spaces previously occupied by Bergmann glial cell cytoplasm. A basket cell (BC) is observed sending its axon (arrowhead) toward the Purkinje cell soma. The arrows indicate a partial view of Purkinje cell infraganglionic plexus. Gold-palladium coating (Castejón and Caraballo (1980a).

FIGURE 15. Sagittally cryofractured cerebellar cortex of a teleost fish showing the elongated Purkinje cell body (PC), its axon hillock region and the axonal initial segment (arrows). A partial view of Purkinje cell infraganglionic plexus (arrowheads) is also seen. A small neuron, presumably a Lugaro cell (LC) is observed at the lower left corner of the figure. A climbing fiber (CF) is also distinguished. Gold-palladium coating. (Castejón and Caraballo (1980a).

FIGURE 16. A-I. Confocal laser scanning microscopy of a Z series of a Purkinje cell (PC) showing at E and F the initial axon segment. Granule (GR), Golgi (GO) and Lugaro (LC) cells also are noted. The arrows point out the climbing fibers ascending toward the Purkinje cell, and molecular layer (ML) layer. (Castejón and Sims, 1999).

ture according with Uchizono hypothesis (Uchizono, 1965,1967). (Fig. 18).

The Purkinje cell recurrent axonal collaterals also contribute to the formation of supra- and infraganglionic plexuses above and below of Purkinje cell layer. Collaterals of Purkinje cell axons form synapses with



FIGURE 17. Purkinje cell myelinated axon (PAx) in the granular layer showing the myelin sheath (MS), circular profiles of smooth endoplasmic reticulum (SER), and mitochondria (M). (Castejón, 2010).

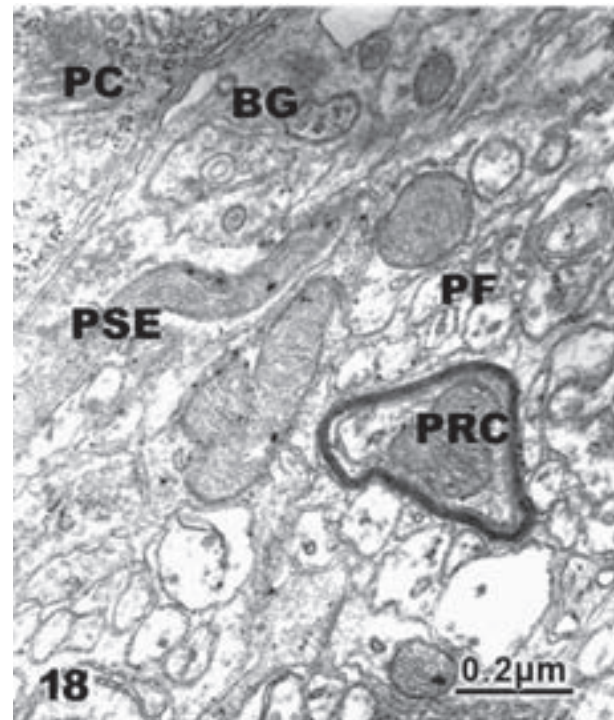


FIGURE 18. Mouse cerebellar molecular later. A myelinated Purkinje recurrent axonal collateral (PRC) is seen surrounded by parallel fibers (PF) and glial cell processes. A Purkinje cell recurrent axonal synaptic ending (PSE) containing flattened vesicles is observed in the vicinity of Purkinje cell soma (PC), and a Bergmann glial cell cytoplasm (BG). Synaptic densities are not visualized (Castejón, 2010).

basket, Golgi cells, and Lugaro cells (Eccles *et al.*, 1967), and with other Purkinje cells (Hamori and Szentágothai, 1968; Lemkey-Johnston and Larramendi, 1968a, b; Larramendi and Lemkey-Johnston, 1979). The terminal arborization of Purkinje cell axons pass into the vestibular or cerebellar nuclei. The reader is referred to the excellent monograph of Ito (1984) for a detailed description of Purkinje cell axons and their relationship with cerebellar nuclei.

Electron microscopy investigation of mouse Purkinje cell axons revealed the existence of a septal reticulum in axonal collaterals of Purkinje cells corresponding to bundles of tubular structures (Castejón, 2010). (Fig. 19).

It was shown that this reticular arrangement of tubular structures may act as a calcium deposit serving the local regulation of cytoskeletal rearrangements (Kiiashchenko and Severina, 1993).

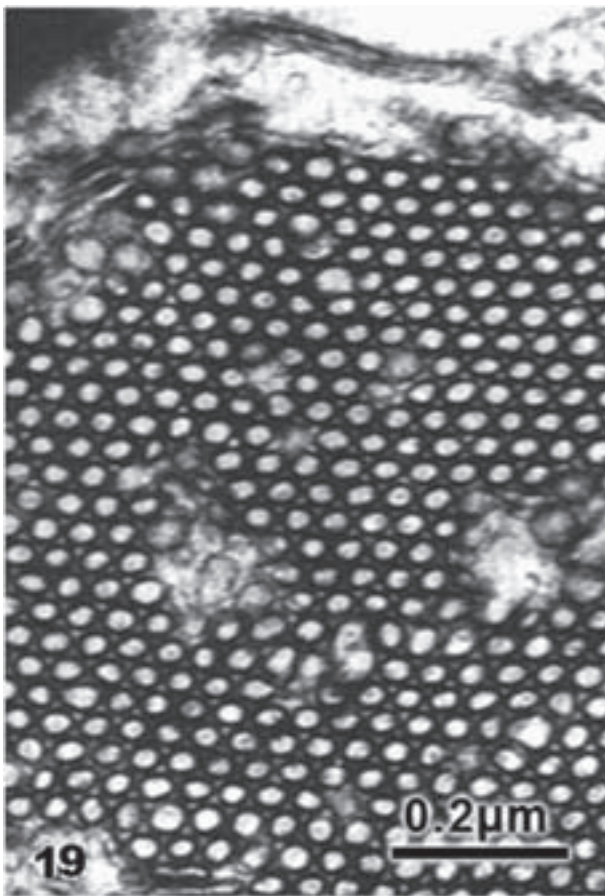


FIGURE 19. Mouse cerebellar cortex. Purkinje cell axonal initial segment exhibiting the characteristic arrangement of cross sections of bundles of tubular profiles (Castejón, 2010).

The pinceau

This is a cerebellar structure formed by descending GABA-ergic basket cell axonal terminals converging on the initial axonal segment of Purkinje cell. As shown in Fig. 15, the outer surface of the pinceau can be imaged with conventional scanning electron microscopy (Castejón, 1988; Castejón, 2003a).

The electrical activity of pinceau contributes to the control of the cerebellar cortical output through the Purkinje cell axon by generating an inhibitory field effect. According to Bobik *et al.* (2004), the abundance of potassium channels and AQP4 localized to cerebellar pinceaux suggests rapid ionic dynamics in the pinceau, and the unusual, highly specialized morphology of this region implies that the structural features may combine with the molecular composition to regulate the microenvironment of the initial segment of Purkinje cell axon. Voltage-activated sodium channels

were not detected in the pinceau, but were localized to the Purkinje cell axon initial segment (Laube *et al.*, 1996).

Purkinje pericellular nest

At transmission electron microscope level, the Purkinje cell soma appears surrounded by the axonal recurrent and basket terminal synaptic endings, and the enveloping Bergmann glial cell cytoplasm (Fig. 20). The descending and transverse axonal collaterals of basket cells contribute to the formation of the enveloping Purkinje cell pericellular basket (Castejón, 1990b).

Transmission electron microscopy shows that the synaptic contacts formed by basket cell axonal collaterals on Purkinje cell soma are characterized by the presence of flat and ellipsoidal synaptic vesicles (Castejón *et al.*, 2001c), characteristic of inhibitory synapses.

At SEM level climbing fibers are also observed forming a pericellular plexus around the Purkinje cell body. They cross the granular layer and reach the Purkinje cell perikaryon contributing to the formation of infraganglionic plexus and pericellular nest (Castejón, 1983). (Figs. 21-24).

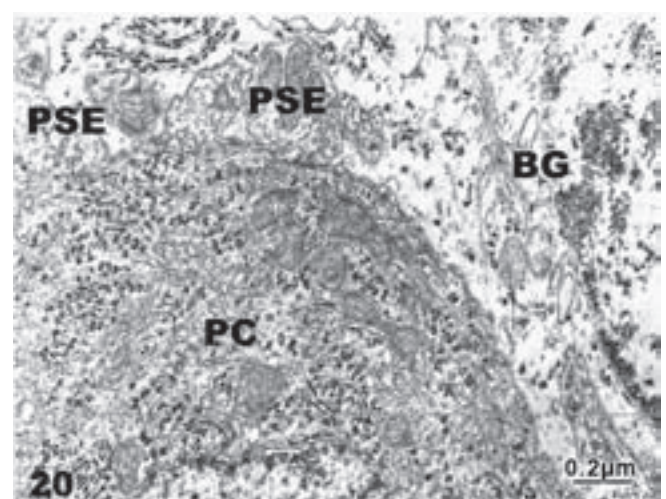


FIGURE 20. Mouse cerebellar cortex. Basket and Purkinje cell axonal recurrent synaptic endings (PSE) making axosomatic contacts with Purkinje cell body (PC). The Bergmann glial cell soma (BG) is observed intimately applied to Purkinje cell (Castejón, 1990b).

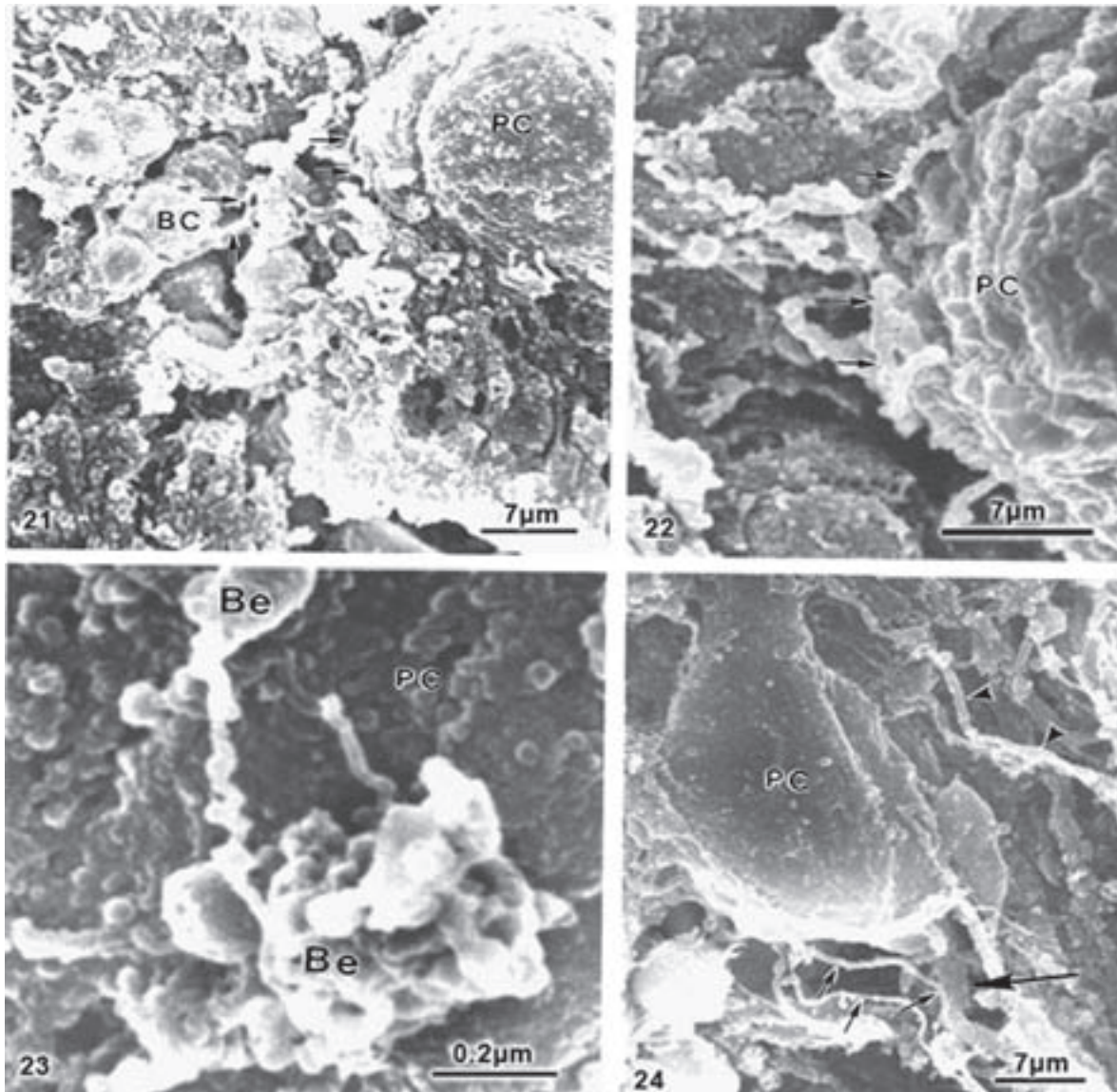


FIGURE 21. Scanning electron micrograph of human cerebellum. Ethanol-cryofracturing technique. A basket cell (BC) located in the Purkinje cell layer is observed giving off its transverse axonal ramifications (arrows) toward a neighboring Purkinje cell (PC). (Castejón and Castejón, 2001c).

FIGURE 22. Scanning electron micrograph of human cerebellum. Ethanol-cryofracturing technique. Higher magnification of the pericellular nest formed by basket cell axonal collaterals (arrows) around Purkinje cell body (PC). The ethanol-cryofracturing technique removed the satellite Bergmann glial cell cytoplasm covering the Purkinje cell soma allowing the visualization of Purkinje cell basket. (Castejón and Castejón, 2001c).

FIGURE 23. Scanning electron micrograph of human cerebellum. Ethanol-cryofracturing technique. Higher magnification showing round and oval interconnected basket cell axonal synaptic endings (BE) applied to the outer surface of Purkinje cell soma (PC). (Castejón, and Castejón, 2001c).

FIGURE 24. Scanning electron micrograph of teleost fish cerebellar cortex. The descending axonal collaterals of a basket cell (short arrows) are observed approaching to the initial axonal segment (long arrow) of Purkinje cell (PC) to form the pinceaux. The arrowheads indicate the climbing fibers ascending toward the molecular layer. (Castejón and Castejón, 2001c).

Parallel fiber-Purkinje dendritic spine synapses

The Purkinje dendritic spines (Pds) were first described by Ramón y Cajal (1955a, b) using Golgi light microscopy technique. Palay and Chan-Palay (1974) examined in detail the Pds using transmission electron microscopy ultrathin sections, and high voltage electron microscopy. Harris and Stevens (1988), using serial electron microscopy and three-dimensional reconstruction, studied the dendritic spines of rat cerebellar Purkinje cells. Napper and Harvey (1988) carried out a quantitative study

of the Pds in the rat cerebellum using stereological methods. Castejón (1990) reported a freeze-fracture scanning electron microscopy and comparative freeze-etching study of parallel fiber-Purkinje spine synapses. Castejón and Apkarian (1993) first reported the field emission scanning electron microscopy features of parallel fiber-Purkinje spine synapses.

Research over the past three-decades has described an impressive mutability in dendritic spine number and morphology under a variety of physiological and pathological circumstances (Shepherd, 1988; Wenisch, *et al.*,

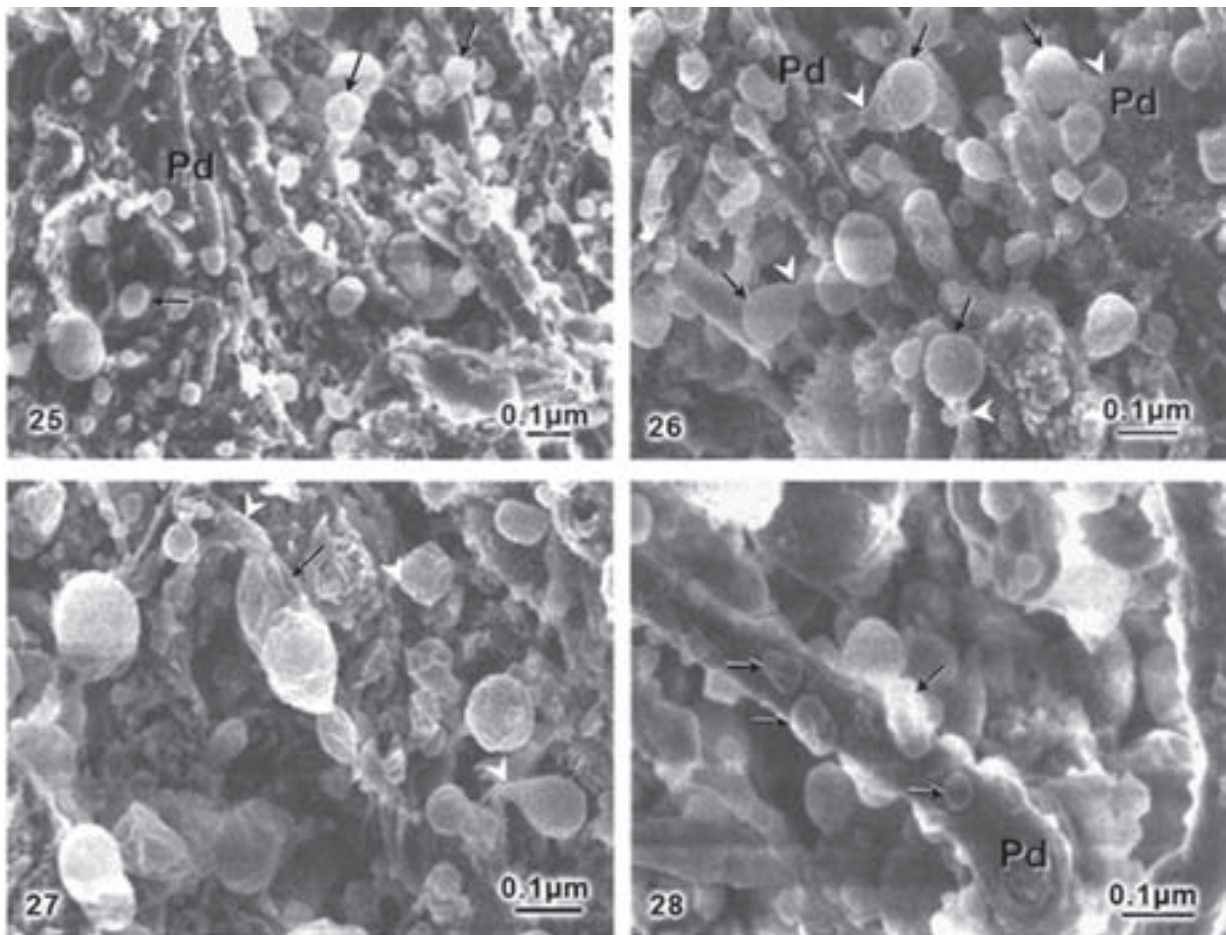


FIGURE 25. Low magnification FESEM of cryofractured mouse cerebellar cortex at the level of outer third molecular layer showing the tertiary ramifications of Purkinje dendrites (Pd) and the outer surface of dendritic spine heads (arrows). Chromium coating. (Castejón *et al.*, 2004a).

FIGURE 26. Higher magnification FESEM of the cryofractured outer third cerebellar molecular layer illustrating the parent Purkinje (Pd) and the mushroom shaped dendritic spine bodies (arrows) and necks (arrowheads). Chromium coating. (Castejón *et al.*, 2004a).

FIGURE 27. Higher magnification FESEM of outer third cerebellar molecular layer showing the mushroom shaped (short arrow) and lanceolate (long arrow) dendritic spines. The spine necks are indicated by arrowheads. Chromium coating. (Castejón *et al.*, 2004a).

FIGURE 28. Higher magnification of FESEM outer third cerebellar molecular layer showing the outer surface of a parent tertiary Purkinje dendritic branch (Pd) and the mushroom type dendritic spines (arrows) separated for 100 to 500 nm spaces. Chromium coating. (Castejón *et al.*, 2004a).

1998; Halpain, 2000; Segal *et al.*, 2000; Marrs *et al.*, 2001; Dailey, 2002; Castejón, 2003a).

Field emission scanning electron microscopy (FESEM) of the cryofractured outer third mouse cerebellar molecular layer shows the smooth outer surface of unattached mushroom shaped Purkinje dendritic spines (Pds) (Fig. 25). The spine neck ranges about 0.68 to 1 μm in mushroom type-dendritic spines. The spine

head has a maximum axial diameter ranging from 1.13 to 1.5 μm . The spine head transversal diameter was about 1 μm (Fig. 26). The elongated spines exhibit an axial diameter up to 2.82 μm and a transversal diameter of 1.30 μm . The spine density is of 18 dendritic spines per 8 μm^2 . Some Pds exhibited elongated and lanceolate shapes, with a neck of 1 μm in length, and a body of up to 2.82 μm in length in axial diameter and a transversal

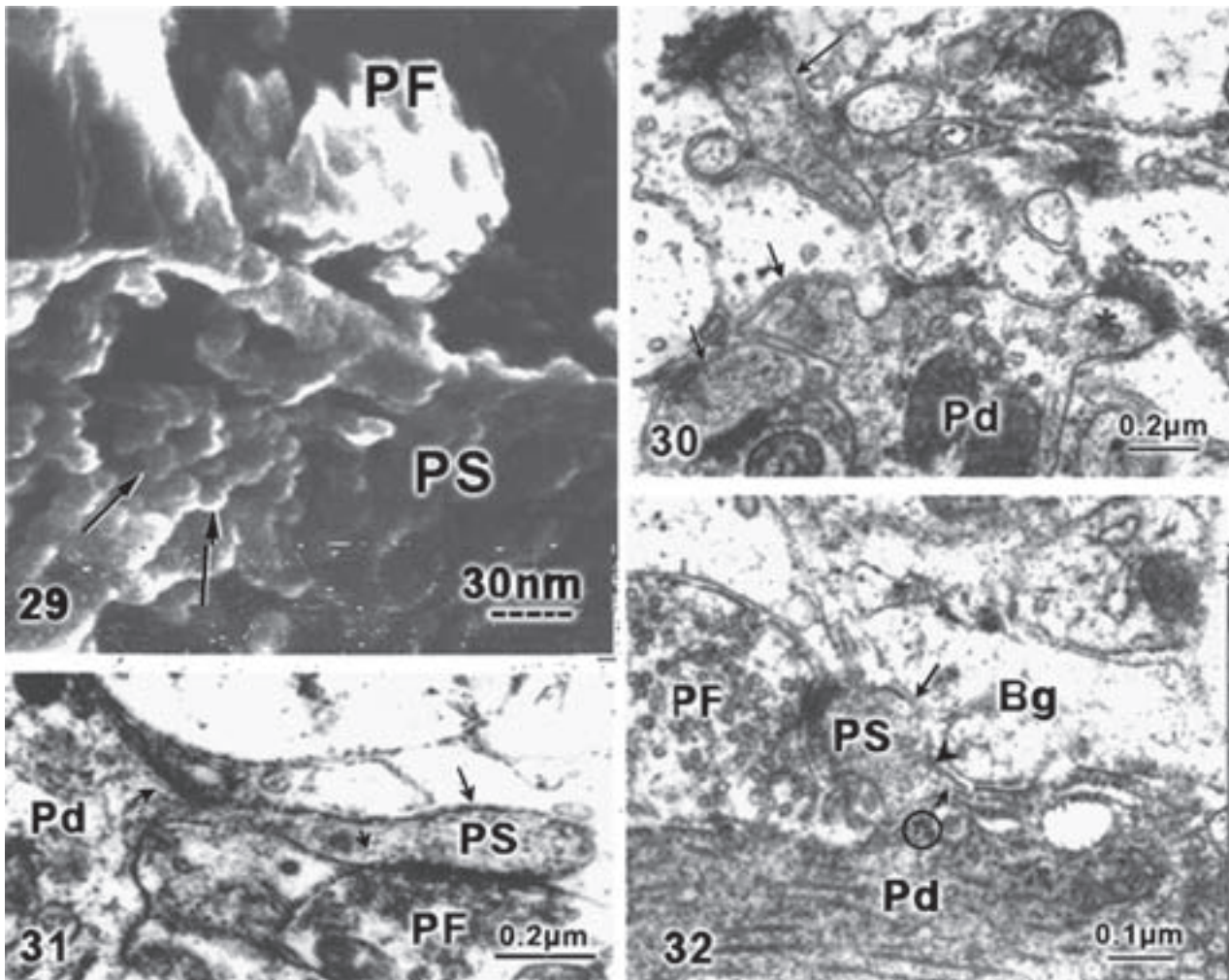


FIGURE 29. High magnification and high resolution FESEM showing the parallel fiber (PF) Purkinje dendritic (PS) spine. The spine postsynaptic membrane exhibits the 25-50 nm globular subunits (arrows). Chromium coating. (Castejón *et al.*, 2001b).

FIGURE 30. Transmission electron micrograph of mouse cerebellar molecular layer depicting the Purkinje dendrite (Pd) giving off long neck elongated spine (long arrow), short neck bulbous spines (short arrows) and stubby or neckless spine (asterisk). Glutaraldehyde-osmium fixed tissue. Uranyl acetate and lead staining (Castejón and Castejón, 1987).

FIGURE 31. Transmission electron micrograph of mouse cerebellar molecular layer showing a parallel fiber (PF)-Purkinje spine (PS) synapse. Note the lanceolate spine containing actin-like filaments (short arrows) and bearing a long neck and an elongated head (long arrow). Pd labels the Purkinje dendritic shaft (Castejón and Castejón, 1997).

FIGURE 32. Transmission electron micrograph of mouse cerebellar molecular layer showing a parallel fiber (PF)-Purkinje spine (PS) synapse. The mushroom type dendritic spine (long arrow) shows actin-like filaments (short arrow), and cluster of free ribosomes (circle) at the site of emergence from the parent dendrite (Pd). The arrowhead points out the short and thick neck. Bg labels the enveloping Bergmann glial cell cytoplasm. (Castejón and Castejón, 1997).

diameter of 1.30 μm (Fig. 27). Close examination of the shaft of a tertiary Purkinje dendritic branch show that the spines are separated by a distance ranging from 50 to 500 μm (Castejón *et al.*, 2004a) (Fig. 28).

The presence of unattached or axonless spines as observed with FESEM could be due to the existence of dendritic spines lacking presynaptic endings (Hirano, 1983; Halpain, 2000), or to an effect produced by the cryofracture method used in the preparative procedure for FESEM. Unattached spines have also been observed after administration of substance P (Baloyannis *et al.*, 1992). Our FESEM images of Purkinje dendritic spines are in agreement with those reported by Harris and Stevens (1988) in rat cerebellar Purkinje cells using serial electron microscopy and three-dimensional reconstruction. Figures 26 and 27 illustrate that neighboring Pds could form a cluster of interacting spines (Shepherd, 1988) especially considering that some spines are separated only by a distance of 50 nm.

Dadonne and Meininger (1975) first reported the scanning transmission electron microscopy features of dendritic spines in the inferior colliculum of cat. Landis and Reese (1983), and Landis *et al.* (1987) showed, in tissue processed by rapid freezing, freeze-fracture and shallow etching, three sets of filamentous structures and globular adherent proteins in cerebellar dendritic spines. Hirano (1983) described unattached spines to any presynaptic ending when granule cells are destroyed before they form the parallel fibers. Wilson *et al.* (1983) reported the three-dimensional structure of dendritic spines in the rat neostriatum using light microscopy and high voltage stereo electron microscopy. Shepherd (1988) postulated that dendritic spines could be related with specific nerve information processing. According to this author, the dendritic spines are structures suitable for rapid local signal processing. This property is related with active sodium and calcium channels.

High magnification field emission scanning electron microscopy shows the synaptic membrane complex of parallel fiber-Purkinje spine synapses, and the 25 to 50 nm globular subunits at the postsynaptic Purkinje dendritic spine, corresponding to the postsynaptic proteins and/ or postsynaptic receptors (Castejón and Apkarian, 1993). (Fig. 29).

Landis and Reese (1974) and Landis *et al.* (1987) earlier described globular adherent proteins at the postsynaptic density. These FESEM images of postsynaptic globular subunits support Landis *et al.* (1987) findings, and the hypothesis of the rapid local signal processing postulated by Shepherd (1988).

Transmission electron microscopy showed bud-like, mushroom-shaped, lanceolate and neckless or stubby spines. (Castejón *et al.*, 2004a). (Fig.30). Some spines exhibit a long neck up to 0.4 μm in length. Lanceolate spines (Fig. 31), making asymmetric synapses with parallel fibers, exhibit an actin-like filament network anchored to a postsynaptic density. Clusters of free ribosomes are observed at the emergence sites of mushroom shaped spines. Purkinje mushroom type dendritic spine synapsing with a parallel fiber are observed in Figure 32.

The wide variety of dendritic-spine shapes, and those observed in the brain sections and neuronal cultures (Van Rossum and Hanisch, 1999) could reflect their current or most-recent activity at a given time. The spine conformational changes could also be related to spine dynamics, as recently observed in confocal scanning laser microscopy (Dailey, 2002) or to spine plasticity (Castejón, 2003b). Such changes could be implicated with associative and motor learning in the cerebellum (Shepherd, 1988; De Zeeuw *et al.*, 1998; Kleim *et al.*, 1998; Van Rossum and Hanisch, 1999; Hansen and Linden, 2000). Spine structural changes are apparently related to variations in calcium ion concentrations (Sabatini *et al.*, 2001), activation of Ca^{++} dependent protein kinases, and the subsequent changes in the spine actin-like and tubulin network (Van Rossum and Hanisch, 1999; Hirai, 2000; Capani *et al.*, 2000). These changes also are related with long term potentiation (LTP) and long term depression (LTD) in the cerebellum (Kim and Linsen, 1999; Halpain, 2000; Segal *et al.*, 2000). Since in our study we are dealing with mature spines, we should consider that changes in the spine morphology could also be correlated mainly with spine plasticity (Haas, 2001; Sala, 2002).

We have reported by means of TEM the presence of an actin filament network occupying the body and neck of Pds, and anchored to the postsynaptic density. Similar filaments were earlier reported by Landis and Reese (1983). In addition, glutamate receptors, predominantly exposed in the dendritic spines of Purkinje cells, are anchored to the actin cytoskeleton. Morphological changes in the actin cytoskeleton regulate delta glutamate receptor clustering and may affect synaptic efficacy and plasticity (Hirai, 2000). According to Fisher *et al.* (2000), glutamate receptors regulate actin-based plasticity in dendrite spines. Haas (2001), considers that as spines mature they become less motile, and AMPA receptors activation now potentiates morphologic stability.

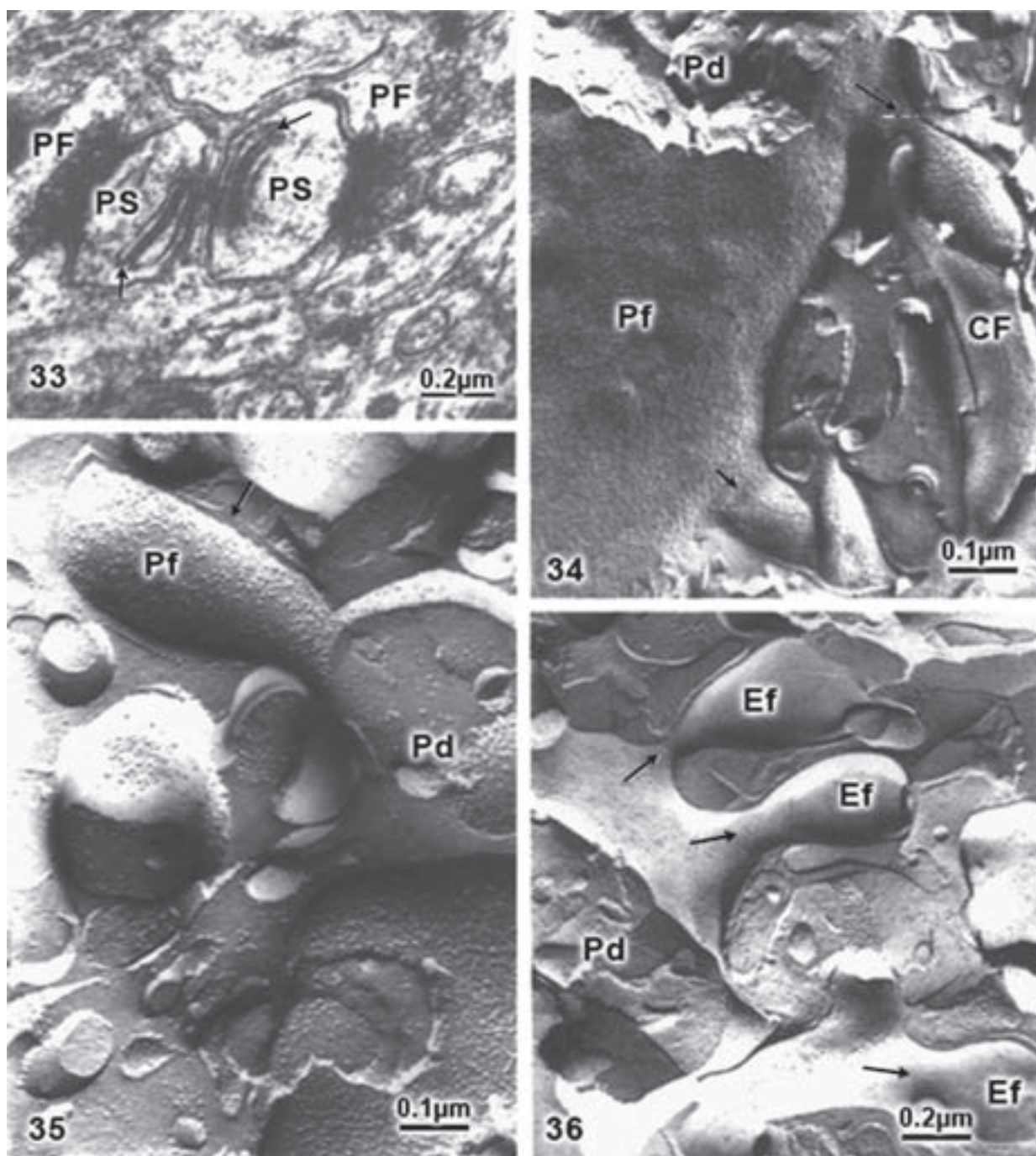


FIGURE 33. Transmission electron micrograph of outer third cerebellar molecular layer showing the cross sections of two neighboring parallel fiber (PF)-Purkinje spine (PS) synapses. The arrows indicate the spine apparatus. (Castejón *et al.*, 2004c).

FIGURE 34. Transmission electron micrograph of a freeze-etching replica of mouse cerebellar molecular layer showing a fractured Purkinje dendrite (Pd). The P face (Pf) of its limiting plasma membrane exhibits the aggregated pattern distribution of intramembrane particles. Note the emergence of a lanceolate spine (long arrow) and the neck of another spine (short arrow). A climbing fiber (CF) is observed establishing contact with the spine neck. Carbon-platinum replica. (Castejón *et al.*, 2004c).

FIGURE 35. Transmission electron micrograph of a freeze-etching replica of mouse cerebellar molecular layer illustrating a fractured Purkinje dendrite (Pd) with a lanceolate spine (arrow). Note the P face (Pf) of spine limiting membrane exhibiting the aggregated pattern distribution of intramembrane particles. Carbon-platinum replica. (Castejón *et al.*, 2004c).

FIGURE 36. Transmission electron micrograph of a freeze-etching replica of mouse cerebellar molecular layer illustrating a fractured Purkinje dendrite (Pd) and the sites of emergence of three neighboring mushroom shaped spines (arrows). The E face (Ef) of the spine membrane shows the classical distribution of isolated particles. (Castejón *et al.*, 2004c).

We have also distinguished elongated or lanceolate spines attached to the presynaptic endings, but not filopodia, as classically described during development (Dailey and Smith, 1996). According to these authors, individual spines undergo shape changes within a timespan of seconds or minutes. Recent reports on the regulation of spine morphology and number lead to the proposal of a unifying hypothesis for a common mechanism involving changes in postsynaptic intracellular Ca^{++} concentration $[Ca^{++}]$. A moderate rise in $[Ca^{++}]$ causes elongation of spines and a very large increase in $[Ca^{++}]$ causes fast shrinkage and eventual collapse of spines (Segal *et al.*, 2000). In addition, high concentration of inositol 1,4,5-trisphosphate 3-kinase has been found in the dendritic spines (Go *et al.*, 1993), which plays crucial role in calcium homeostasis. More recently, Velazquez-Zamora *et al.* (2011) suggest that the development of motor control may be closely linked to the distinct developmental patterns of dendritic spines on Purkinje cells, which has important implications for future studies of cerebellar dysfunctions.

The spine head showed the spine apparatus formed by two or three flattened sacs joined by a cementing and dark electron-dense substance (Fig. 33). The freeze-etching replica method showed the three-dimensional structure and intramembrane morphology of the spines. Figures 34 and 35 illustrate the P face of a fractured Purkinje dendritic branch and their mushroom shape and lanceolate spines, characterized by a uniform and aggregated distribution pattern of intramembrane particles (IMPs). About 90 IMPs were observed in the spine head, and about 65 IMPs at the short neck. The E face of mushroom shaped spines showed about 9 isolated IMPs at the level of the neck and about 35 IMPs at the spine head (Castejón *et al.*, 2004c). (Fig. 36).

The spine apparatus was earlier reported in the dendritic spines of neocortex, endorhinal cortex, hippocampal dentate gyrus and neostriatum, and has been associated with the postsynaptic density (Tarrant and Routtenberg, 1979). In our study we have found clusters of free ribosomes at the base of dendritic spines, which suggest local protein synthesis. Presumably, after their synthesis, proteins are stored in the spine apparatus, to be later transferred to the postsynaptic density.

Fractured dendritic spines establishing synaptic contacts with climbing fiber endings (Fig. 37) show aggregated IMPs at the synaptic active zones, the spine apparatus and profiles of smooth endoplasmic reticulum. Some mushroom type dendritic spines show simultaneous synaptic contacts with climbing fiber endings at both the neck and the head (Fig. 38). In fractured

parallel fiber-Purkinje spine synapses, a tangential view of the spine postsynaptic membrane show the IMPs provided with central hole, corresponding to open postsynaptic ionic channels (Fig. 39). High magnification of a parallel fiber-Purkinje spine synapse (Fig. 40) show the distribution of large, medium, small, and elongated IMPs at the level of the postsynaptic membrane, corresponding with the localization of postsynaptic proteins and/or postsynaptic receptors. This image could be correlated with the FESEM image of globular subunits of the postsynaptic membrane illustrated in Figure 29.

Immunocytochemistry of GluR1 subunit of AMPA receptors

GluR1 is one of the several subunits of the subclass of quisqualate (QA) receptors coupled to cationic ionic channel, also termed AMPA receptors (Morrison *et al.*, 1996; Crepel *et al.*, 1996; Michaelis, 1996; Negyessy *et al.*, 1997). GluR1 immunoreactivity was concentrated along the Purkinje and basket cell bodies and their dendritic arborization (Castejón and Dailey, 2009). Strong immunofluorescent staining was observed surrounding the Purkinje cell bodies corresponding to the enveloping Bergmann glial cell cytoplasm (Castejón, 2011) contributing to the formation of the pericellular nest, and to climbing fibers endings at the level of primary dendritic trunk (Castejón *et al.*, 2000b).

The Purkinje cell dendritic arborization and their spines can also be fully appreciated in low magnification rat cerebellar slices labeled with antibodies against GluR1 subunits of AMPA receptors, and imaged at low magnification with the confocal laser scanning microscope. (Castejón and Dailey, 2009). (Fig. 42).

The GluR1 distribution pattern corresponds mainly with the postsynaptic sites of the excitatory circuits formed by parallel and climbing fiber endings upon Purkinje cells (Castejón and Dailey, 2009). A similar relationship of GluR1 subunits of AMPA receptors with excitatory circuits have also been reported by Morrison *et al.* (1996) in the hippocampus and neocortex. Negyessy *et al.* (1997) demonstrated by light and electron microscopy the presence of mGluR5 metabolic glutamate receptors in rat cerebellar cortex.

Parallel and climbing fibers are likely to use glutamate as neurotransmitter (Ito, 1984; Kano *et al.*, 1988; Zhang *et al.*, 1990; Otis *et al.*, 1997). These two excitatory inputs to Purkinje cells, mediate fast excitatory postsynaptic potentials via AMPA type

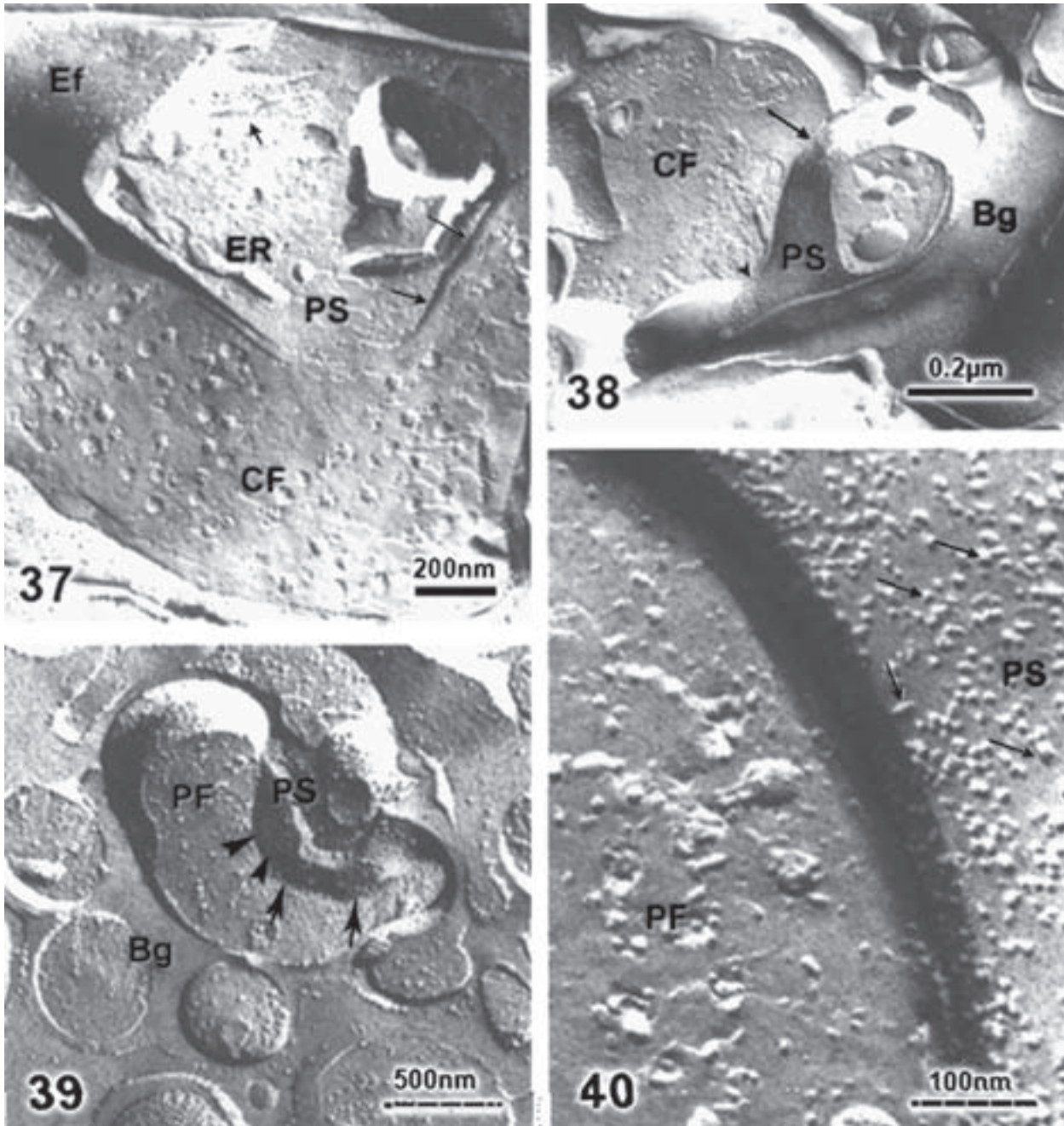


FIGURE 37. Transmission electron micrograph of a freeze-etching replica of mouse cerebellar molecular layer showing a climbing fiber (CF)-Purkinje spine (PS) synapse. The long arrows indicate the synaptic active zone. The spine apparatus (short arrow), and the smooth endoplasmic reticulum (ER) are distinguished in the spine head. The E face (Ef) of the spine neck also is seen (Castejón *et al.*, 2004c).

FIGURE 38. Transmission electron micrograph of a freeze-etching replica of mouse cerebellar molecular layer showing a fractured mushroom type-Purkinje dendrites spine (PS) establishing synaptic contact with a climbing fiber ending (CF). Note that the synaptic active zone includes the neck (arrowhead) and the head (long arrow) of the spine. The Bergmann glial cell membrane (Bg) ensheaths the synaptic contact (Castejón *et al.*, 2004c).

FIGURE 39. Transmission electron micrograph of a freeze-etching replica of mouse cerebellar molecular layer showing a fractured parallel fiber (PF)-Purkinje spine (PS) synapse. The fractured postsynaptic spine membrane (short arrows) exhibits intramembrane particles with a central hole (arrow-leads) corresponding to open ionic channels. The enveloping Bergmann glial cell membrane (Bg) also is seen (Castejón, 1990a).

FIGURE 40. High magnification high resolution freeze etching replica of a parallel fiber (PF)-Purkinje spine (PS) showing the distribution of intramembrane particles at the level of postsynaptic spine membrane. Large, medium, and small globular particles, and elongated ones (arrows) are observed. (Castejón, 1990a).

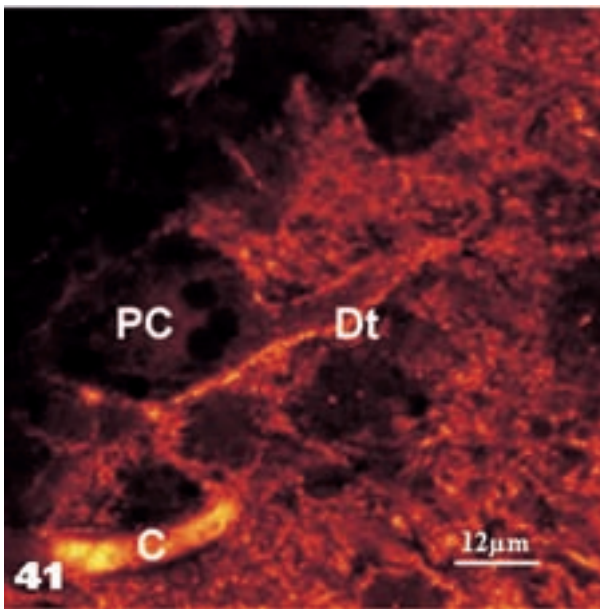


FIGURE 41. Rat cerebellar slice labeled with specific antibody against GluR1 subunit of AMPA receptors showing the immunopositive reaction of Purkinje cell soma (PC) and its primary dendritic trunk (Dt), corresponding to the surrounding Bergmann glial cell cytoplasm, and climbing fiber endings. A capillary (C) also show positive immunolabeling (Castejón and Dailey, 2009).

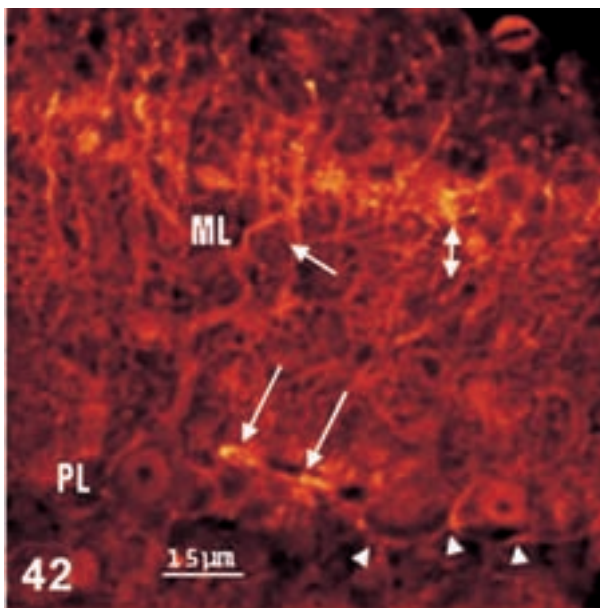


FIGURE 42. Slice of rat cerebellar cortex labeled with specific antibody against GluR1 subunit of AMPA receptors showing the Purkinje cell soma at the Purkinje cell layer (PL), and their dendritic branches at the molecular (ML) layer. Large hotspots clusters are observed surrounding Purkinje cell body (arrowheads). Small puncta (double head arrow) are observed in the outer third molecular layer. The short arrow points out the soma of a stellate neuron. A capillary (long arrows) also is heavily fluorescent. This image represents a composite of 13 image planes spanning a depth of 13 μm. (Castejón and Dailey, 2009).

ionotropic glutamate receptors (Knöpfel and Grandes, 2002). The AMPA receptors of Purkinje cells are indeed involved in induction and expression of long-term depression (Crepel *et al.*, 1996), and in cerebellar synaptic plasticity (Kano and Kato, 1987; Kano *et al.*, 1988). More recently, Piochon *et al.* (2010) suggest that the late developmental expression of postsynaptic NMDA receptors at CF synapses onto Purkinje cells is associated with a switch toward an NMDA receptor-dependent LTD induction mechanism.

N-cadherin immunohistochemistry

N-cadherin is a membrane glycoprotein mediating strong homophilic adhesion and concentrated at the synaptic junctions and neural circuits, where they exert an active role in synaptic structure, function, plasticity, and in selective interneuronal connections during network function (Redies, 1995, 1997, 2000; Redies and Takeichi, 1996; Suzuki *et al.*, 1991; Tang *et al.*, 1998; Obst-Pernberg and Redies, 1999; Huntley and Benson, 1999; Tanaka *et al.*, 2000; Togashi *et al.*, 2002; Huntley *et al.*, 2002).

Purkinje cell soma and dendritic ramifications show strong punctate immunostaining in rat cerebellar slices double labeled with a primary antibody against N-

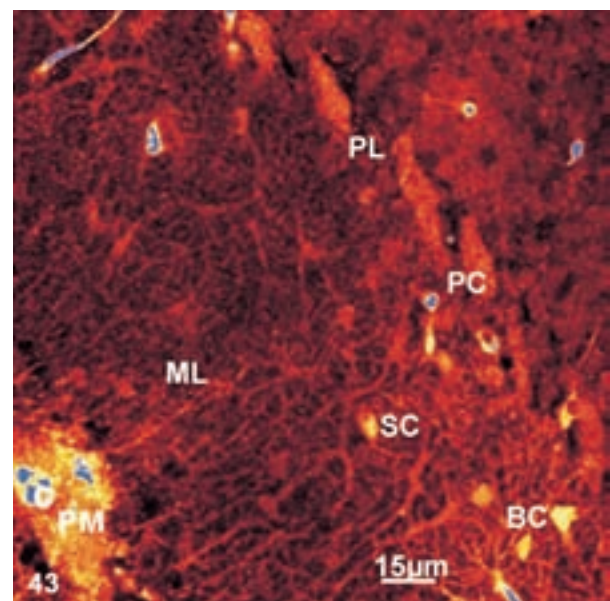


FIGURE 43. Rat cerebellar slices double labeled with a primary antibody against N-cadherin, and Alexa 488 goat anti mouse (GAM)-antibody. The Purkinje cell layer (PL) shows a row of immunoreactive Purkinje cells (PC), and their dendritic ramifications. Note the strong immunostaining of stellate (SC) and basket cells (BC) in the molecular layer, and capillaries (C) at the level of the cerebellar pia mater (PM). (Castejón, 2010).

cadherin, and Alexa 88 goat anti mouse (GAM)-antibody. (Fig. 43). The punctate immunostaining of Purkinje cell secondary and tertiary dendritic branches corresponds to parallel fiber-Purkinje dendritic spine synapses (Castejón, 2010).

The N-cadherin immunoreactivity observed at the Purkinje pericellular nest corresponds to the axosomatic synapses of basket cell axonal endings upon Purkinje cells earlier described at transmission electron microscopy level (Hámori and Szentágothai, 1965; Mugnaini, 1972; Palay and Chan-Palay, 1974; Castejón and Castejón, 2001). The strong punctate immunoreactivity observed at the whole thickness of molecular layer corresponds to the climbing fiber-Purkinje cell spine synapses (Hámori and Szentágothai, 1965; Mugnaini, 1972; Palay and Chan-Palay, 1974; Castejón and Sims, 2000; Castejón *et al.*, 2000b), to the parallel fiber synapses with Purkinje cell dendritic spines (Hámori and Szentágothai, 1965; Palay and Chan-Palay, 1974; Castejón, 1990; Castejón and Apkarian, 1993; Castejón and Castejón, 1997; Castejón *et al.*, 2001b).

Immunohistochemistry of Ca²⁺/calmodulin-dependent protein kinase II alpha

Calcium/calmodulin-dependent protein kinase II (CaMKII) is a Ca²⁺-activated enzyme that is highly abundant in the brain and plays a major role in Ca²⁺-mediated signal transduction (Tokumitsu *et al.*, 1995; Nakamura *et al.*, 1996). CaMKII constitutes a family of multifunctional protein kinase isoforms (alpha, beta, gamma and delta) starting in prenatal development (Jensen *et al.*, 1991). CaMKII beta isoform is the major subunit present in the cerebellum (Sola *et al.*, 1999; Chang *et al.*, 2001). CaMKII alpha and beta isoforms also are expressed in the cerebellum of jaundiced Gunn rats during development (Conlee *et al.*, 2000). The precise neuronal and synaptic localization of CaMKII alpha isoform in the granular, Purkinje and molecular layers of developing and mature rat cerebellar cortex have not been established.

Clear evidence of staining of Purkinje cell nuclei is not observed. Stacks of up to 28 optodigital sections at the molecular layer show small punctate staining spreaded throughout the whole thickness of the molecular layer, corresponding to parallel fiber-Purkinje spine synapses. Punctate staining surrounding Purkinje cell primary dendritic trunk also is found, corresponding to the localization of climbing fiber-Purkinje dendritic spine synapses. Bergmann glial cell bodies and their radial fibers did not exhibit CaMKII

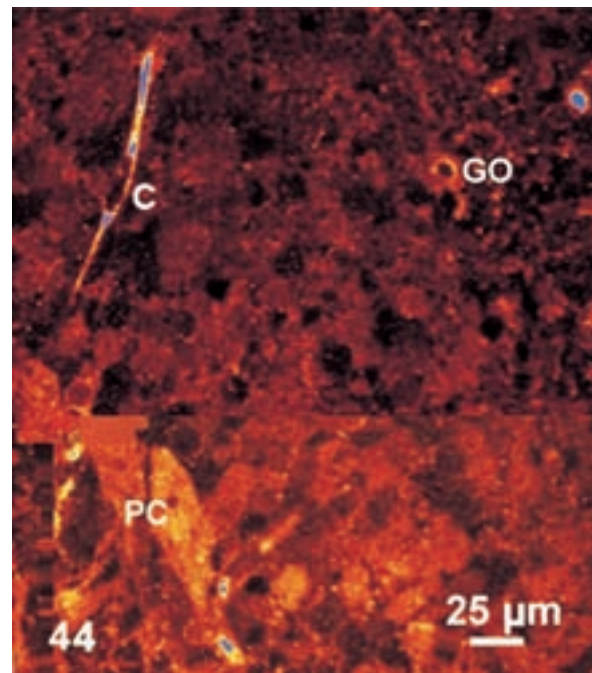


FIGURE 44. Rat cerebellar slice double labeled with a primary antibody against CaMKII alpha, and a secondary antibody the Alexa 488 goat anti mouse (GAM)-antibody. Strong immunostaining is observed at Purkinje cell body (PC), Golgi cell (GO), and a capillary (C). (Castejón, 2010).

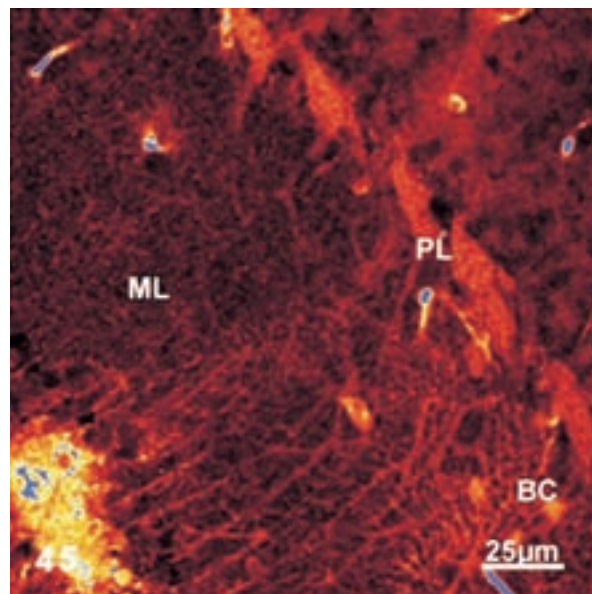


FIGURE 45. Rat cerebellar slice, double labeled with a primary antibody against CaMKII alpha, and a secondary antibody the Alexa 488 goat anti mouse (GAM)-antibody. Positive immunoreactivity is observed at the Purkinje cell layer (PL), and their dendritic ramification in the molecular layer (ML), and basket cell (BC). (Castejón, 2010).

alpha immunoreactivity. Close examination at the level of Purkinje cell layer show the CaMKII alpha strong immunoreactivity of basket cell axonal ending contributing to the formation of Purkinje cell pericellular nest (Figs. 44 and 45). (Castejón, 2010).

Calcium/calmodulin-dependent protein kinase II (CaMKII) is a prominent enzyme in mammalian brain capable of phosphorylating a variety of substrate proteins (Ouimet *et al.*, 1984). CaMKII is an enzyme that plays a major role in the regulation of long-term potentiation, a form of synaptic plasticity associated with learning and memory (Jin *et al.*, 1999; Nakamura *et al.*, 1996; Lisman *et al.*, 2002).

Previous studies by means of biochemical methods, electron microscopy and confocal laser scanning microscopy have localized the CaMKII at the level of postsynaptic density (Yamauchi and Yoshimura, 1998; Lisman *et al.*, 2002), being central to the regulation of glutamatergic synapses. According to Lisman *et al.* (2002) recent work indicates that a binding pattern for CaMKII is the NMDA receptor within the postsynaptic density. The AMPA receptor subunit GluR1 is also phosphorylated by CaMKII enhancing channel function. The CaMKII has been postulated by Lisman *et al.* (2002) as a molecular switch for long-term information storage, and serving as a molecular basis of long-term synaptic memory. Furthermore, activation of the NMDA receptor in cerebellar granule cells activated CaMKII (Fujunaga and Soderling, 1990).

CaMKII alpha presence in the main excitatory and inhibitory circuits of developing cerebellar cortex is presumably related with its participation in information, and motor learning and memory processes. Our findings support the role of CaMKII as a molecular switch that is capable of storing long-term synaptic memory (Lisman *et al.*, 2002).

Synapsin- I and PSD-95 immunohistochemistry

Rat cerebellar slices labeled with synapsin I show immunoreactivity of basket cell endings surrounding Purkinje cell body, and of climbing fibers surrounding the primary dendritic trunk, as well as parallel fibers with Purkinje secondary and tertiary dendritic ramifications (Castejón, 2010). (Fig. 46).

Double labelling using calbindin and PSD-95 show a low magnification the calcium content of Purkinje cell body and processes. The PSD-95 labels the postsynaptic receptor localization at the Purkinje cell body and dendritic branching (Fig. 48a,b). (Castejón *et al.*, 2004b).

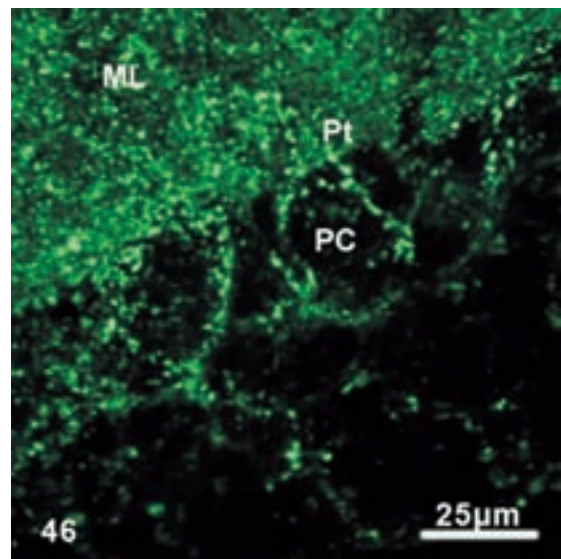


FIGURE 46. Rat cerebellar cortex labeled with synapsin-I depicting the green perineuronal net formed by the presynaptic endings of basket cell axons upon Purkinje cell body (PC), and the small puncta surrounding the Purkinje primary dendritic trunk (Pt), corresponding mainly to climbing fiber presynaptic endings, and with parallel fiber-Purkinje secondary and tertiary dendritic branches in the molecular layer (ML). (Castejón, 2010).

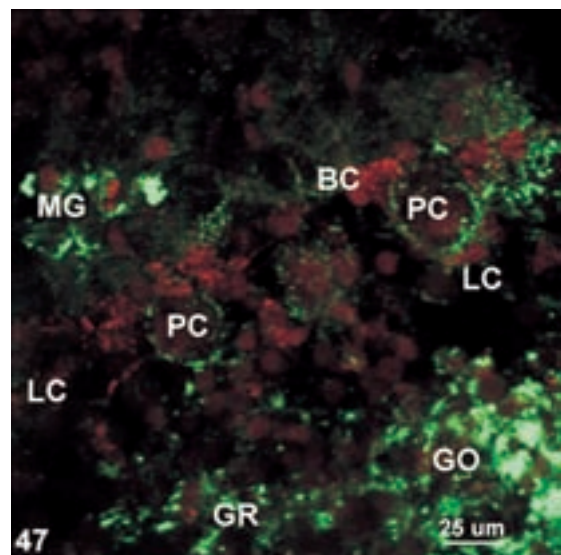


FIGURE 47. Rat cerebellar slice double labelled with synapsin-I and PSD-95 exhibiting as small green puncta the immunoreactivity of presynaptic endings of climbing fibers and basket cell axons with the Purkinje cell soma forming part of the pericellular nest. The red patches correspond to the postsynaptic endings of basket (BC), granule (GR), Golgi (GO), and Lugaro cells (LC). The green patches correspond to mossy and climbing fiber glomerular regions (GR) in the granular layer. Some immunopositive synapsin-I ectopic glomeruli (MG) are observed in the molecular layer (Castejón, 2010).

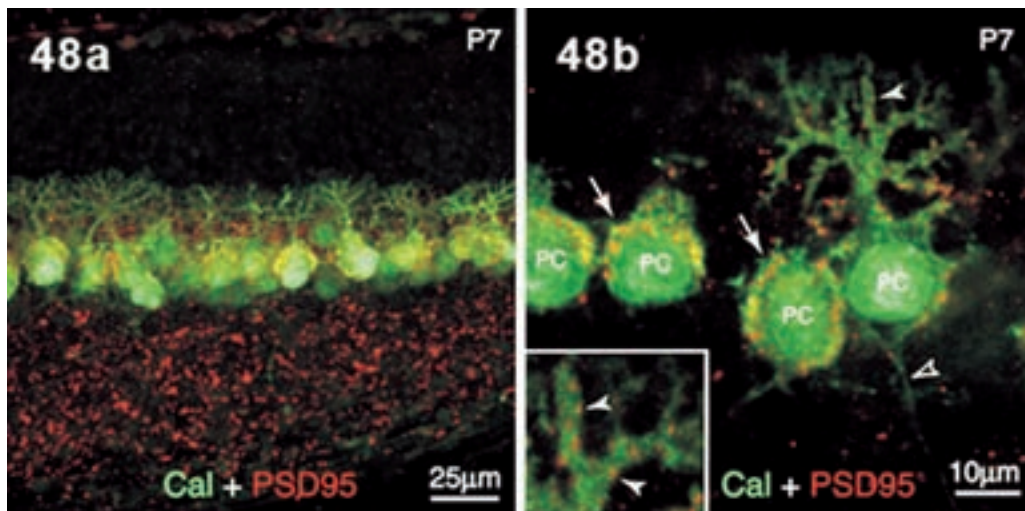


FIGURE 48. a. Rat cerebellar cortex double labelled with calbindin (green) and PSD-95 (red). b. The arrows indicate the Purkinje cell (PC) perineuronal net formed mainly by basket cell axons. The arrowheads at the inset point out the postsynaptic receptors of parallel fibers-Purkinje dendritic branches. The arrowhead label Purkinje cell axons. Note the numerous red puncta labeling the postsynaptic receptors at the granular layer corresponding mainly to the mossy fibers, granule cells and Golgi dendrites (Castejón *et al.*, 2004b).

Concluding remarks

Correlative microscopy of Purkinje cell made by means of light microscopy, transmission electron microscopy and freeze-etching technique, scanning electron microscopy and cryofracture method, field emission scanning electron microscopy, confocal laser scanning microscopy and the use of Methamorph image analysis, as well as the use of immunohistochemical techniques for confocal laser scanning microscopy have permitted a better and deeper understanding of cerebellar structure and function, mainly regarding the three-dimensional morphology of outer neuronal surface, intramembrane morphology, Purkinje cell synaptic contacts, both axospinodendritic and axosomatic contacts. The use of immunohistochemical techniques for Synapsin-I and PSD-95, and GluR1 subtype of AMPA receptors have allowed us to disclose the localization of pre- and postsynaptic receptors. Purkinje cell positive immunoreactivity for N-cadherin and CaMKII alpha subtype also have being demonstrated.

References

- Alvarez-Otero R, Regueira SD, Anadon R (1993). New structural aspects of the synaptic contacts on Purkinje cell in an elastomeric cerebellum. *Journal of Anatomy* **182**: 13-21.
- Arnett CE, Low FN (1985). Ultrasonic microdissection of rat cerebellum for scanning electron microscopy. *Scanning Electron Microscopy* **1**: 274-255.
- Avruschenko MSh, Marshak TL (1983). Dark and clear Purkinje's cells in the cerebellum during the postresuscitation period. *Biulleten' eksperimental'noi biologii i meditsiny* **95**: 105-108.
- Baloyannis SJ, Costa V, Deretzi GJ (1992). Intraventricular administration of substance P induces unattached Purkinje cell dendritic spines in rats. *International Journal of Neuroscience* **62**: 251-262.
- Banno T, Kohno K (1998). Conformational changes of the smooth endoplasmic reticulum are facilitated by L-glutamate and its receptors in rat Purkinje cells. *Journal of Comparative Neurology* **402**: 252-263.
- Bardo S, Robertson B, Stephens GJ (2002). Presynaptic internal Ca²⁺ stores contribute to inhibitory neurotransmitter release onto mouse cerebellar Purkinje cells. *British Journal of Pharmacology* **137**: 529-537.
- Bernocchi G, Barni S, Biggiogera M (1986). Electron-cytochemical localization of succinic semialdehyde dehydrogenase activity in Purkinje neurons and hepatocytes of the rat. *Journal of Neuroscience Methods* **17**: 31-42.
- Bertoni-Freddari C, Fattoretti P, Casoli T, Gracciotti N, Solazzi M, Pompei P (2001). Quantitative cytochemical mapping of mitochondrial enzymes in rat cerebella. *Micron* **32**: 405-410.
- Bielschowski M, Wolff M (1904). Zur Histologie der Kleinhirnrinde. *Journal of Psychology*. **4**: 1-23.
- Bobik M, Ellisman MH, Rudy B, Martone ME (2004). Potassium channel subunit Kv3.2 and the water channel aquaporin-4 are selectively localized to cerebellar pinceau. *Brain Research* **1026**: 168-178.

- Bosel'ová L, Ochodnická E, Magdolenová S, *et al.* (1978). The Golgi apparatus of pale and dark Purkinje cells. *Folia Morphologica (Praha)* **26**: 257-259.
- Buchanan RA, Leapman RD, O'Connell MF, Reese TS, Andrews SB (1993). Quantitative scanning transmission electron microscopy of ultrathin cryosections: subcellular organelles in rapidly frozen liver and cerebellar cortex. *Journal of Structural Biology* **110**: 244-255.
- Capani E, Martone ME, Deerinck TJ (2000). Selective localization of high concentrations of F-actin in subpopulations of dendritic spines in rat central nervous system: a three-dimensional electron microscopic study. *Journal of Comparative Neurology* **435**: 156-170.
- Cardell M, Landsend AS, Eidet J (2003). High resolution immunogold analysis reveals distinct subcellular compartmentation of protein kinase C gamma and delta in rat Purkinje cells. *Neuroscience* **82**: 709-725.
- Castejón OJ (1968). Electron microscopic observations at the cerebellar molecular layer. *Investigación Clínica* **27**: 57-108.
- Castejón HV, Castejón OJ (1972). Application of Alcian Blue and OS-DMEDA in the electron histochemical study of the cerebellar cortex. *Revista de Microscopía Electrónica y Biología Celular* **1**: 207-225.
- Castejón HV, Castejón OJ (1976). Electron microscopic demonstration of hyaluronidase sensible proteoglycans at the presynaptic area in mouse cerebellar cortex. *Acta Histochemica (Jena)* **55**: 300-316.
- Castejón OJ, Caraballo AJ (1980a). Light and scanning electron microscopy study of cerebellar cortex of Teleost fish. *Cell & Tissue Research* **207**: 211-226.
- Castejón OJ, Caraballo AJ (1980b). Application of cryofracture and SEM to the study of human cerebellar cortex. *Scanning Electron Microscopy* **4**: 197-207.
- Castejón, OJ, Valero C (1980). Scanning electron microscopy of human cerebellar cortex. *Cell & Tissue Research* **212**: 363-374.
- Castejón OJ, Castejón HV (1981). Transmission and scanning electron microscopy and ultracytochemistry of vertebrate and human cerebellar cortex. In: *Glial and Neuronal Cell Biology*. (Fedoroff, S. Ed.), p. 249-258, Alan R. Liss Inc. New York.
- Castejón OJ (1983). Scanning electron microscope recognition of intracortical climbing fiber pathways in the cerebellar cortex. *Scanning Electron Microscopy* **3**: 1427-1434.
- Castejón OJ, Castejón HV (1987). Electron microscopy and glycosaminoglycan histochemistry of cerebellar stellate neurons. *Scanning Electron Microscopy* **1**: 681-693.
- Castejón OJ (1988). Scanning electron microscopy of vertebrate cerebellar cortex. *Scanning Electron Microscopy* **2**: 569-597.
- Castejón OJ (1990a). Freeze-fracture scanning electron microscopy and comparative freeze-etching study of parallel fiber-Purkinje spine synapses of vertebrate cerebellar cortex. *Journal of Submicroscopic Cytology & Pathology* **22**: 281-295.
- Castejón OJ (1990b). Surface and membrane morphology of Bergmann glial cells and their topographic relationships in the cerebellar molecular layer. *Journal of Submicroscopic Cytology & Pathology* **22**: 123-134.
- Castejón OJ, Castejón HV (1991). Three-dimensional morphology of cerebellar protoplasmic islands and proteoglycans content of mossy fiber glomerulus: A scanning and transmission electron microscope study. *Scanning Electron Microscopy* **5**: 477-494.
- Castejón OJ, Apkarian RP (1992). Conventional and high resolution scanning electron microscopy of outer and inner surface features of cerebellar nerve cells. *Journal of Submicroscopic Cytology & Pathology* **24**: 549-562.
- Castejón OJ, Apkarian RP. (1993). Conventional and high resolution field emission scanning electron microscopy of vertebrate cerebellar parallel fiber-Purkinje spine synapses. *Cellular Molecular Biology (Noisy-le-Grand)* **39**: 863-873.
- Castejón OJ, Castejón HV, Apkarian RP (1994). High resolution scanning electron microscopy features of primate cerebellar cortex. *Cellular Molecular Biology (Noisy-le-Grand)* **40**: 1173-1181.
- Castejón OJ, Castejón HV (1997). Conventional and high resolution scanning electron microscopy of cerebellar Purkinje cells. *Biocell* **21**: 149-159.
- Castejón OJ, Sims P (1999). Cytoarchitectonic arrangement and intracortical circuits of hamster cerebellum. A study by means of confocal laser scanning microscopy. *Biocell* **23**: 187-196.
- Castejón OJ, Sims P (2000). Three-dimensional microscopy of cerebellar climbing fibers. A study by means of light microscopy, confocal laser scanning, microscopy and scanning and transmission electron microscopy. *Scanning Electron Microscopy* **22**: 211-217.
- Castejón OJ, Castejón HV, Sims P (2000a). Confocal, scanning and transmission electron microscopic study of cerebellar mossy fiber glomeruli. *Journal of Submicroscopic Cytology & Pathology* **32**: 247-260.
- Castejón OJ, Castejón HV, Alvarado MV (2000b). Further observations on cerebellar climbing fibers. A study by means of light microscopy, confocal laser scanning microscopy and scanning and transmission electron microscopy. *Biocell* **24**: 197-212.
- Castejón OJ, Apkarian RP, Castejón HV (2001a). Field emission scanning electron microscopy and freeze-fracture transmission electron microscopy of mouse cerebellar synaptic contacts. *Journal of Submicroscopic Cytology & Pathology* **33**: 289-300.
- Castejón OJ, Castejón HV, Apkarian P (2001b). Confocal laser scanning and scanning and transmission electron microscopy of vertebrate cerebellar granule cells. *Biocell* **25**: 235-255.
- Castejón OJ, Castejón HV (2001c). Correlative microscopy of cerebellar basket cells. *Journal of Submicroscopic Cytology & Pathology* **33**: 23-32.
- Castejón OJ (2003a). Purkinje cells. In: *Scanning Electron Microscopy of Cerebellar Cortex*. Kluwer Academic/ Plenum Publisher. New York, pp 57-67.
- Castejón OJ (2003b). Synaptic plasticity in the oedematous human cerebral cortex. *Journal of Submicroscopic Cytology & Pathology* **35**: 177-197.
- Castejón OJ, Castellano A, Arismendi G (2004a). Correlative microscopy of Purkinje dendritic spines. A field emission scanning and transmission electron microscopic study. *Journal of Submicroscopic Cytology & Pathology* **36**: 29-36.
- Castejón OJ, Leah T, Dailey M (2004b). Localization of synapsin and PSD-95 in developing postnatal rat cerebellar cortex. *Developmental Brain Research* **151**, 25-32.
- Castejón OJ, Castellano A, Arismendi G (2004c). Transmission electron microscopy study of cortical dendritic spines in the human oedematous cerebral cortex. *Journal of Submicroscopic Cytology and Pathology* **36**: 181-191.

- Castejón OJ (2008). Ultrastructural pathology of Golgi apparatus of nerve cells in human brain edema. In: *Electron Microscopy of Human Brain Edema*. Astrodata. Maracaibo. Venezuela, p 47-54.
- Castejón OJ, Dailey ME (2009). Immunohistochemistry of Glur1 subunits of AMPA receptors of rat cerebellar nerve cells. *Biocell* **33**: 71-78.
- Castejón OJ (2010). Purkinje cells. In: *Comparative and Correlative Microscopy of Cerebellar Cortex*. Astrodata. Venezuela. p 99-120.
- Castejón OJ. (2011). Correlative microscopy of cerebellar neuroglial cells. *Journal of Advanced Microscopy Research* **6**: 159-176.
- Chang BH, Mukherji S, Soderling TR (2001). Calcium/calmodulin-dependent protein kinase II inhibitor protein: localization of isoforms in rat brain. *Neuroscience* **102**: 767-777.
- Chan-Palay V, Palay S (1971). The synapse "en marron" between Golgi II neurons and mossy fiber in the rat's cerebellar cortex. *Z Anat Entwickl Gesch.* **133**: 274-287.
- Chan-Palay V (1971). The recurrent collaterals of Purkinje cell axons. A correlated study of the rat's cerebellar cortex with electron microscopy and the Golgi method. *Zeitschrift für Anatomie und Entwicklungsgeschichte* **134**: 200-234.
- Conlee JW, Shapiro SM, Churn SB (2000). Expression of the alpha and beta subunits of Ca²⁺/calmodulin kinase II in the cerebellum of jaundiced Gunn rats during development: a quantitative light microscopic analysis. *Acta Neuropathologica* **99**: 393-401.
- Crepel F, Hemart H, Jaillard D, Daniel H (1996). Cellular mechanism of long-term depression in the cerebellum. *Behavioral & Brain Science* **19**: 347-353.
- Crevatin J (1898). Ueber die Zellen von Fusari und Ponti im Kleinhirn von Säugetieren. *Anatomischer Anzeiger* **14**: 25-38.
- Dadonne JP, Meininger V (1975). Scanning transmission electron microscopy of dendritic spines stained by the Golgi method. *Comptes Rendus Hebdomadaires des Séances de l'Académie des Sciences. D. Sciences Naturelles* **280**: 2669-2672.
- Dailey ME, Smith SJ (1996). The dynamics of dendritic structure in developing hippocampal slices. *Journal of Neuroscience* **16**: 2983-2994.
- Dailey ME (2002). Optical imaging of neural structure and physiology: Confocal microscopy in live brain slices. In: *Brain Mapping: The Methods*. Elsevier Science, New York, USA, p. 49-76.
- Denissenko J (1877). Zur frage über den Bau der Kleinhirnrinde bei den verschiedenen Klassen von Wirbeltieren. *Archiv für mikroskopische Anatomie* **14**: 203-242.
- De Zeeuw CI, Simpson JI, Hoogenraad CC, Galjart N, Koekkoek SK, Ruigrok TJ (1998). Microcircuitry and function of the inferior olive. *Trends in Neuroscience* **21**: 391-400.
- Dogiel L (1896). Die Nervenlemente in Kleinhirnrinde der Vogel und Säugethiere. *Archiv für mikroskopische Anatomie* **47**: 707-719.
- Dröscher A (1998). Camilo Golgi and the discovery of Golgi apparatus. *Histochemistry and Cell Biology* **109**: 425-430.
- Eccles JC, Ito M, Szentágothai J (1967). Purkinje cells. In: *The Cerebellum as a Neuronal Machine*. New York. Springer-Verlag, p 1-145.
- El-Dwairi QA (2007). Two subpopulations of human Purkinje neurons: an electron microscopy study. *Neuroendocrinology Letters* **28**: 247-249.
- Estable C (1923). Notes sur la structure comparative de l'écorce cérébelleuse, et dérivées physiologiques possibles. *Trabajos del Laboratorio de Investigaciones Biológicas* (Madrid) **21**: 169-265.
- Fisher M, Kaech S, Wagner U, Brinhaus H, Matus A (2000). Glutamate receptors regulate actin-based plasticity in dendritic spines. *Nature Neuroscience* **3**: 887-894.
- Fox CA, Barnard JW (1957). A quantitative study of the Purkinje cell dendritic branchlets and their relationship to afferent fibers. *Journal of Anatomy (Lond.)* **91**: 299-313.
- Fox CA (1962). Fine structure of the cerebellar cortex. In: *Correlative Anatomy of the Nervous System*. (Crosby EC, Humphreys T, Lauer EW. Eds.), MacMillan Co., New York. USA. p. 192-198.
- Fox CA, Siegesmund KA, Dutta CR (1964). The Purkinje cell dendritic branchlets and their relation with the parallel fibers: light and electron microscopic observations. In: *Morphological and Biochemical Correlates of Neural Activity* (Cohen MM, Snider RS. Eds.), Hoeber-Harper and Row. New York, p. 1112-1141.
- Fox CA, Hillman DE, Siegesmund KA, Dutta CR (1967). The primate cerebellar cortex. A Golgi and electron microscopic study. *Progress in Brain Research* **25**: 174-225.
- Fujunaga K, Soderling TR (1990). Activation of Ca²⁺/calmodulin-dependent protein kinase II in cerebellar granule cells by N-methyl-D-aspartate receptor activation. *Molecular and Cellular Neuroscience* **1**: 3270-3277.
- Gao HL, Feng WY, Li XL, Hu H, Huang L, Wang ZY (2009). Golgi apparatus localization of ZNT7 in the mouse cerebellum. *Histology & Histopathology* **24**: 567-572.
- Garcia-Segura LM, Perrelet A (1984). Postsynaptic membrane domains in the molecular layer of the cerebellum: a correlation between presynaptic inputs and postsynaptic plasma membrane organization. *Brain Research* **321**: 255-256.
- Go M, Uchida T, Takazawa, Endo T, Erneux C, Mailleux P, Onaya T (1993). Inositol 1,4,5-trisphosphate 3-kinase highest levels in the dendritic spines of cerebellar Purkinje cells and hippocampal CA1 pyramidal cells. A pre- and post-embedding immunoelectron microscopic study. *Neuroscience Letters* **158**: 135-138.
- Göbel W, Helmchen F (2007). New angles on neuronal dendrites *in vivo*. *Journal of Neurophysiology* **98**: 3770-3779.
- Golgi C (1882). Sulla fina anatomia degli organi centrali del sistema nervoso. I Nota preliminari sulla struttura, morfologia e vicendevoli rapporti delle cellule ganglionare. *Rivista Sperimentale di Freniatria* **8**: 165-195.
- Golgi C (1886). Sulla fina anatomia degli organi centrali del sistema nervoso. *Rivista Sperimentale di Freniatria* **11**: 31-45.
- Gray EG (1961). The granule cells, mossy synapses and Purkinje spine synapses of the cerebellum: Light and electron microscope observations. *Journal of Anatomy* **95**: 345-356.
- Haas K (2001). Old spines can't dance. *Trends in Neuroscience* **24**: 7.
- Halpain S (2000). Acting and the agile spine: how and why do dendritic spines dance? *Trends in Neuroscience* **23**: 141-146.
- Hamori J, Szentágothai J (1964). The "crossing-over" synapses: An electron microscope study of the molecular layer on the cerebellar cortex. *Acta Biologica Academiae Scientiarum Hungaricae* **15**: 95-117.
- Hamori J, Szentágothai J (1965). The Purkinje cell baskets: Ultrastructure of an inhibitory synapse. *Acta Biologica Academiae Scientiarum Hungaricae* **15**: 465-479.

- Hamori J, Szentágothai J (1968). Identification of synapses formed in the cerebellar cortex by Purkinje axon collaterals: an electron microscopic study. *Experimental Brain Research* **15**: 118-128.
- Hansen C, Linden DJ (2000). Long-term depression of the cerebellar climbing fiber-Purkinje neuron synapse. *Neuron* **26**: 473-483.
- Harris KM, Stevens JK (1988). Dendritic spines of rat cerebellar Purkinje cells: serial electron microscopy with reference to their bio-physic characteristics. *Journal of Neuroscience* **8**:4435-4459.
- Held J (1897). Beiträge zur Struktur der Nervenzellen und ihrer Fortsätze. *Archiv für Anatomie und Physiologie. Anatomische Abteilung (Suppl)*, **3**: 273-342.
- Herndon RM (1963). The fine structure of Purkinje cell. *Journal of Cell Biology* **18**:167-180.
- Hirai H (2000). Clustering of delta glutamate receptors is regulated by the activity of cytoskeleton in the dendritic spines of cultured rat Purkinje cells. *European Journal of Neuroscience* **12**: 563-570.
- Hirano A (1983). The normal and aberrant development of synaptic structures between parallel fibers and Purkinje cell dendritic spines. *Journal of Neural Transmission (Suppl)* **18**: 1-8.
- Hojo T (1994). An experimental scanning electron microscopic study of human cerebellar cortex using t-butyl alcohol freeze-drying device. *Scanning Electron Microscopy* **8**: 303-313.
- Humphreys WJ, Spurlock BO, Johnson JS (1975). Transmission electron microscopy of tissue prepared for scanning electron microscopy of tissue prepared by ethanol-cryofracturing technique. *Stain Technology* **50**: 119-125.
- Huntley GW, Benson DL (1999). Neural (N)-cadherin at developing thalamocortical synapses provides an adhesion mechanism for the formation of somatopically organized connections. *Journal of Comparative Neurology* **407**: 453-471.
- Huntley GW, Gil O, Bozdagi O (2002). The cadherin family of cell adhesion molecules: multiple roles in synaptic plasticity. *Neuroscientist* **8**: 221-233.
- Ige AO, Bolam JP, Billinton A, White JH, Marshall FH, Emson PC (2000). Cellular and subcellular localisation of GABA(B1) and GABA (B2) receptor proteins in the rat cerebellum. *Brain Research. Molecular Brain Research* **83**: 72-80.
- Ito M (1984). Purkinje cells In: *The Cerebellum and Neural Control*. Raven Press. New York, p 21-115.
- Jakob A (1928). Das Kleinhirn. In: *Handbuch der mikroskopischen Anatomie des Menschen*. Vol. IV. (Mollendorff WV, Ed.) Julius Springer. Berlin. p 771-831.
- Jensen KF, Ohmstede CA, Fisher RS, Sahyoun N (1991). Acquisition and loss of a neuronal Ca²⁺/calmodulin-dependent protein kinase during neuronal differentiation. *Proceedings of the National Academy of Sciences (USA)* **88**: 4050-4053.
- Jin JK, Choi JK, Lee HG, Kim Y, Carp RI, Choi EK (1999). Increased expression of CaM Kinase II alpha in the brains of scrapie infected mice. *Neuroscience Letters*. **273**: 37-40.
- Kanaseki T, Ikeuchi Y, Tashiro Y (1998). Rough surfaced smooth endoplasmic reticulum in rat and mouse cerebellar Purkinje cells visualized by quick-freezing techniques. *Cell Structure & Function* **23**: 373-387.
- Kano M, Kato M (1987). Quisqualate receptors are specifically involved in cerebellar synaptic plasticity. *Nature* **325**: 276-279.
- Kano M, Makoto K, Chang HS (1988). The glutamate receptor subtype mediating parallel fibre-Purkinje cell transmission in rabbit cerebellar cortex. *Neuroscience Research* **5**: 325-337.
- Khan MA (1993). Histochemical and ultrastructural investigation of heterogeneous Purkinje neurons in mammalian cerebellum. *Cell & Molecular Biology Research* **39**: 789-795.
- Kiiashchenko LI, Severina IJU (1993). The structural-functional organization of the endoplasmic reticulum in the neurons of the rat cerebellar cortex. *Zhurnal evoliutsionnoi biokhimi i fiziologii* **29**: 398-401.
- Kim CH, Linsen JE (1999). A role of actin filament in synaptic transmission and long-term potentiation. *Journal of Neuroscience* **19**: 4314-4324.
- Kleim JA, Swain RA, Armstrong KA (1998). Selective synaptic plasticity within the cerebellar cortex following complex motor skill learning. *Neurobiology of Learning & Memory* **69**: 274-289.
- Knöpfel T, Grandes P (2002). Metabotropic glutamate receptors in the cerebellum with a focus on their function in Purkinje cells. *The Cerebellum* **1**: 19-26.
- Kölliker A (1890). Zur feineren Anatomie des zentralen Nervensystems; I. Das Kleinhirn *Zeitschrift für wissenschaftliche Zoologie* **49**: 663-689.
- Lache H (1906). Sur les corbeilles des cellules de Purkinje. *Comptes Rendus de la Societé de Biologie (Paris)* **9**: 10-18.
- Landis D, Reese RS (1974). Differences in membrane structure between excitatory and inhibitory synapses in the cerebellar cortex. *Journal of Comparative Neurology* **155**: 93-126.
- Landis DM, Reese TS (1983). Cytoplasmic organization in cerebellar dendritic spines. *Journal of Cell Biology* **97**: 1169-1178.
- Landis DM, Weinstein LA, Reese TS (1987). Substructure in the postsynaptic density of Purkinje cell dendritic spines revealed by rapid freezing and etching. *Synapse* **1**, 552-558.
- Larramendi LMH, Lemkey-Johnston N (1979). The distribution of recurrent Purkinje collateral synapses in the mouse cerebellar cortex: an electron microscopic study. *Journal of Comparative Neurology* **138**: 451- 482.
- Laube G, Röper J, Pitt JC, Sewin S, Kistner U, Garner CC, Pongs O, Weh RW (1996). Ultrastructural localization of Shaker-related potassium channel subunits and synapse-associated protein 90 to septate-like junctions in rat cerebellar Pinceaux. *Brain Research. Molecular Brain Research* **42**:51-61.
- Lemkey-Johnston N, Larramendi LMH (1968a). Morphological characteristics of mouse stellate, basket cells and their neuroglial envelope: An electron microscopic study. *Journal of Comparative Neurology* **134**:39-72.
- Lemkey-Johnston N, Larramendi LMH (1968b). Types and distribution of synapses upon basket and stellate cells of the mouse cerebellum. *Journal of Comparative Neurology* **134**: 73-112.
- Lisman J, Schulman H, Cline H (2002). The molecular basis of CaMKII function in synaptic and behavioural memory. *Nature Reviews in Neuroscience* **13**:175-190.
- Loesch A, Glass R (2006). Electron microscopy and in situ hybridization: Expression of P2Y2 receptor mRNA in the cerebellum. *Methods in Molecular Biology* **326**: 151-162.
- Marrs GS, Green Sh, Dailey ME (2001). Rapid formation and remodelling of postsynaptic densities in developing dendrites. *Nature Neuroscience* **4**: 1006-1013.
- Martone ME, Zhang Y, Simpliciano VM, Carrasqher BO, Elishman MH (1993). Three-dimensional visualization of the smooth endoplasmic reticulum in Purkinje cell dendrites. *Journal of Neuroscience* **13**: 4636-4646.
- Mateos JM, Azkue J, Sarria R, Kuhn RH, Grandes P, Knöpfel T (1998). Localization of the mGlu4a metabotropic glutamate receptor in rat cerebellar cortex. *Histochemistry & Cell Biology* **109**:135-139.

- Matsumura A, Kohno K (1991). Microtubule bundles in fish cerebellar Purkinje cells. *Anatomy & Embryology* **183**:105-110.
- Mashimo M, Hirabayashi T, Murayama T, Shimizu T (2008). Cytosolic PLA2(alpha) activation in Purkinje neurons and its role in AMPA-receptor trafficking. *Journal of Cell Science* **121**: 3015-3024.
- Meek J, Nieuwenhuys R (1991). Palisade pattern of mormyrid Purkinje cells: a correlated light and electron microscopic study. *Journal of Comparative Neurology* **306**:156-192.
- Meller K (1987). The cytoskeleton of cryofixed Purkinje cells of the chicken cerebellum. *Cell & Tissue Research* **247**: 155-165.
- Michaelis EK (1996). Glutamate neurotransmission: Characteristics of NMDA receptors in the mammalian brain. *Neural Notes* **2**: 3-6.
- Miller KK, Verma A, Snyder SH, Ross CA (1991). Localization of an endoplasmic reticulum calcium ATPase mRNA in rat brain by in situ hybridization. *Neuroscience* **43**: 1-9.
- Monteiro RA (1991). Genesis, structure and transit of dense bodies in rat neocerebellar cortical cells, namely Purkinje neurons: an ultrastructural study. *Journal für Hirnforschung* **32**: 593-609.
- Monteiro RA, Rocha E, Marini-Abreu MM (1994). Heterogeneity and death of Purkinje cells of rat neocerebellum (Crus I and Crus II): hypothetic mechanisms based on qualitative and quantitative microscopical data. *Journal für Hirnforschung* **35**: 205-222.
- Morrison JH, Siegel SJ, Gazzaley AH, Kordower JH, Mufson EJ (1996). Glutamate receptors: Emerging links between subunit proteins and specific excitatory circuits in primate hippocampus and neocortex. *The Neuroscientist* **2**: 272-283.
- Mugnaini E (1972). The histology and cytology of the cerebellar cortex. In: *The Comparative Anatomy and Histology of the Cerebellum. The Human Cerebellum. Cerebellar Connections and Cerebellar Cortex*. (Larsell O, Jansen J. Eds). The University of Minnesota Press, Minneapolis, p. 201-251.
- Nakamura Y, Okuno S, Kitani T, Okate K, Sato F, Fujisawa H (1996). Distribution of Ca²⁺/calmodulin-dependent protein kinase alpha in the rat central nervous system: an immunohistochemical study. *Neuroscience Letters* **204**: 61-64.
- Napper RM, Harvey RJ (1988). Quantitative study of the Purkinje cell dendritic spines in the rat cerebellum. *Journal of Comparative Neurology* **274**: 158-167.
- Negyessy L, Vidnyanszky Z, Kuhn R, Knöpfel T, Görc TJ, Hamori J (1997). Light and electron microscopic demonstration of mGluR5 metabotropic glutamate receptor immunoreactive neuronal elements in the rat cerebellar cortex. *Journal of Comparative Neurology* **385**: 641-650.
- Novikoff AB (1967). Enzyme localization and ultrastructure of neurons. In: *The Neuron*. (Hyden H, Ed.), Elsevier. New York. p 255-238.
- Obst-Pernberg K, Redies C (1999). Cadherins and synaptic specificity. *Journal of Neuroscience Research* **58**: 130-138.
- Opdam FJ, Echard A, Croes HJ, van den Hurk JA, van de Vorstenbosch RA, Ginsel LA, Goud B, Franssen JA (2000). The small GTPase Rab6B, a novel Rab6 subfamily member, is cell-type specifically expressed and localised to the Golgi apparatus. *Journal of Cell Science* **113**: 2725-2735.
- Otis TS, Kavanaough MP, Jahr CE (1997). Postsynaptic glutamate transport at the climbing fiber-Purkinje cell synapse. *Science* **277**: 1515-1518.
- Ottersen OP, Madsen S, Storm-Mathisen J, Somogyi P, Scopsi L, Larsson LI (1988a). Immunocytochemical evidence suggests that taurine is colocalized with GABA in the Purkinje cell terminals, but that the stellate cell terminals predominantly contain GABA: a light- and electronmicroscopic study of the rat cerebellum. *Experimental Brain Research* **72**: 407-416.
- Ottersen OP, Storm-Mathisen J, Somogyi P (1988b). Colocalization of glycine-like and GABA-like immunoreactivities in Golgi cell terminals in the rat cerebellum: a postembedding light and electron microscopic study. *Brain Research* **450**:342-353.
- Ouimet CC, Mc Guinness TL, Greengard P (1984). Immunocytochemical localization of calcium/calmodulin-dependent protein kinase II in rat brain. *Proceedings of the National Academy of Sciences (USA)* **81**: 5604-5608.
- Palay SL, Palade GE (1955). The fine structure of neurons. *Journal of Biophysical and Biochemical Cytology* **1**: 69-88.
- Palay SL, Chan-Palay V (1974). Purkinje cells. In: *Cerebellar Cortex. Cytology and Organization*. Springer-Verlag, Berlin, p. 11-62.
- Paulus W, Lehr A, Peiffer, Markovic A, Wiedmann KH (1990). Immunohistochemical demonstration of mitochondria in routinely processed tissue using a monoclonal antibody. *Journal of Pathology* **160**: 321-328.
- Peterson M, Leblond CP (1964). Synthesis of complex carbohydrates in Golgi region, as shown by autoradiography after injection of labeled glucose. *Journal of Cell Biology* **21**: 143-148.
- Piochon C, Levenes C, Ohtsuki G, Hansel C (2010). Purkinje cell NMDA receptors assume a key role in synaptic gain control in the mature cerebellum. *J of Neuroscience* **30**:15330-15335.
- Purkinje JE (1837). Neueste Untersuchungen aus der Nerven und Hirn Anatomie. In: *Bericht über die Versammlung deutscher Naturforscher und Aertze in Prag*. (Stenberg K, von Krombholz JV, Eds). p 177-180.
- Ramón y Cajal S (1890). A propos de certains éléments bipolaires du cervelet avec quelques détails nouveau sur l'évolution des fibres cérébelleuses. *Internationale Monatschrift für Anatomie und Physiologie* **7** : 447-468.
- Ramón y Cajal S (1955a). Purkinje cells. In: *Histologie du Système Nerveux de l'Homme et des Vertébrés* Vol. 2. Consejo Superior de Investigaciones Científicas, Instituto Ramón y Cajal. Madrid, p. 1-54.
- Ramón y Cajal S (1955b). Grandes células etoílées ou células de Golgi. In: *Histologie du Système Nerveux de l'Homme et des Vertébrés*. Consejo Superior de Investigaciones Científicas. Instituto Ramón y Cajal. Madrid. p 79-105.
- Redies C (1995). Cadherin expression in the developing vertebrate CNS: from neuromeres to brain nuclei and neural circuits. *Experimental Cell Research* **220**: 243-256 .
- Redies C, Takeichi M (1996). Cadherins in the developing central nervous system: an adhesive connection for segmental and functional subdivisions. *Developmental Biology* **180**: 413-423.
- Redies C (1997). Cadherins and the formation of neural circuitry in the vertebrate CNS. *Cell & Tissue Research* **290**: 405-413.
- Redies C (2000). Cadherins in the central nervous system. *Progress in Neurobiology* **61**: 611-648.
- Retzius V (1892). Die nervösen Elemente der Kleinhirnrinde. *Biologische Untersuchungen* **3**: 17-29.
- Ross CA, Meldolesi J, Milner TA, Satoh T, Supattapone S, Snyder SH (1989). Inositol 1,4,5-trisphosphate receptor localized to endoplasmic reticulum in cerebellar Purkinje neurons. *Nature* **339**: 468-470.

- Rusakov DA, Podini P, Villa A, Villa A, Meldolesi J (1993). Tridimensional organization of Purkinje neuron cisternal stacks, a specialized endoplasmic reticulum subcompartment rich in inositol 1,4,5-trisphosphate receptors. *Journal of Neurocytology* **22**: 273-282.
- Sabatini B, Maravall M, Svobod KA (2001). Ca(2+) signalling in dendritic spines. *Current Opinion in Neurobiology* **11**: 349-356.
- Sala C (2002). Molecular regulation of dendritic spine shape and function. *Neurosignals* **11**: 213-223.
- Sandonà D, Scolari A, Mikoshiba K, Volpe P (2003). Subcellular distribution of Homer 1b/c in relation to endoplasmic reticulum and plasma membrane proteins in Purkinje neurons. *Neurochemistry Research* **28**: 1151-1158.
- Scheibel AB, Paul L, Fried I (1981). Scanning electron microscopy of the central nervous system. I. The cerebellum. *Brain Research Reviews* **3**: 207-228.
- Segal M, Korkotian E, Murohy DD (2000). Dendritic spine formation and pruning: common cellular mechanisms? *Trends in Neuroscience* **23**: 53-57.
- Shepherd GM (1988). Purkinje cells. In: *The Synaptic Organization of the Brain*. Oxford University Press, New York, p. 1-19.
- Shinonaga Y (1962). Lysosomes and pigment granules. I. Purkinje cells of the rat cerebellum. *Archivum Histologicum Japonicum* **22**: 377-385.
- Shiomura Y, Hirokawa N (1987). The molecular structure of microtubule-associated protein 1A (MAP1A) *in vivo* and *in vitro*. An immunoelectron microscopy and quick-freeze, deep-etch study. *Journal of Neuroscience* **7**: 1461-1469.
- Smirnov AE (1897). Über eine besondere von Nervenzellen der Molecularschicht des Kleinhirn bei erwachsenen Säugetieren und beim Menschen. *Anatomischer Anzeiger* **13**: 636-642.
- Sola C, Tusell JM, Serratos J (1999). Comparative study of the distribution of calmodulin kinase II and calcineurin in the mouse brain. *Journal of Neuroscience Research* **57**: 651-662.
- Sotelo C (1969). Ultrastructural aspects of the cerebellar cortex of the frog. In: *Neurobiology of Cerebellar Evolution and Development*. (Linás R., Ed). Med Assn/Educ & Res Fnd Chicago, p 327-371.
- Suzuki S, Sano K, Tanihara H (1991). Diversity of the cadherin family: evidence for eight new cadherins in nervous tissue. *Cell Regulation* **2**: 261-270.
- Takahashi-Iwanaga H (1992). Reticular endings of Purkinje cell axons in the rat cerebellar nuclei: scanning electron microscopic observations of the pericellular plexus of Cajal. *Archives of Histology & Cytology* **55**: 307-314.
- Tanaka H, Shan W, Phillips GR, Arndt K, Bozdagi O, Shapiro L, Huntley GW, Benson DL, Colman DR (2000). Molecular modification of N-cadherin in response to synaptic activity. *Neuron* **25**: 93-107.
- Tang L, Hung CP, Schuman EM (1998). A role for the cadherin family of cell adhesion molecules in hippocampal long-term potentiation. *Neuron* **20**: 1165-1175.
- Tarrant SB, Routtemberg A (1979). Postsynaptic membrane and spine apparatus: proximity in dendritic spines. *Neuroscience Letters* **11**: 289-294.
- Terasaki M, Slater NT, Fein A, Schmidek A, Reese TS (1994). Continuous network of endoplasmic reticulum in cerebellar Purkinje neurons. *Proceedings of the National Academy of Sciences (USA)* **91**: 7510-7514.
- Tewari HB, Bourne GH (1963). Histochemical studies on the "Dark" and "Light" cells of the cerebellum of the rat. *Acta Neuropathologica* **3**: 1-15.
- Togashi H, Abe K, Mizoguchi A, Takaoka K, Chisaka O, Takeichi M (2002). Cadherin regulates dendritic spine morphogenesis. *Neuron* **35**: 77-89.
- Tokumitsu H, Enslin H, Soderling TR (1995). Characterization of CA2+/calmodulin-dependent protein kinase cascade, molecular cloning and expression of calcium/calmodulin-dependent protein kinase. *Journal of Biological Chemistry* **270**: 19320-19324.
- Uchizono K (1965). Characteristics of excitatory and inhibitory synapses in the central nervous system of the cat. *Nature* **207**: 642-643.
- Uchizono K (1967). Synaptic organization of the Purkinje cells in the cerebellum of the cat. *Experimental Brain Research* **4**: 97-113.
- Van Rossum D, Hanisch UK (1999). Cytoskeletal dynamics in the dendritic spine: direct modulation by glutamate receptors? *Trends in Neuroscience* **22**: 290-295.
- Velázquez-Zamora DA, Martínez-Degollado M, González-Burgos I (2011). Morphological development of dendritic spines on rat cerebellar Purkinje cells. *International Journal of Developmental Neuroscience* **5**: 515-520.
- Villa A, Sharp AH, Racchetti G, Podini P, Bole DG, Dunn WA, Pozzan T, Snyder SH, Meldolesi J (1992). The endoplasmic reticulum of Purkinje neuron body and dendrites: molecular identity and specializations for Ca2+ transport. *Neuroscience* **49**: 467-477.
- Walton PD, Airey JA, Sutko JL, Beck CF, Mignery GA, Südhof TC, Deerinck TJ, Ellisman MH (1991). Ryanodine and inositol trisphosphate receptors coexist in avian cerebellar Purkinje neurons. *Journal of Cell Biology* **113**: 1145-1157.
- Wenisch S, Fortmann B, Steinmetz T, Kriete A, Leiser R, Bitsch I (1998). 3-D confocal laser scanning microscopy used in morphometric analysis of rat Purkinje cell dendritic spines after chronic ethanol consumption. *Anatomy, Histology & Embryology* **27**: 393-397.
- Wilson CJ, Groves PM, Kitai ST, Linder JC (1983). Three-dimensional structure of dendritic spines in the rat neostriatum. *Journal of Neuroscience* **3**: 383-388.
- Yamamoto A, Otsu H, Yoshimori T, Maeda N, Mikoshiba K, Tashiro Y (1991). Stacks of flattened smooth endoplasmic reticulum highly enriched in inositol 1,4,5-trisphosphate (InsP3) receptor in mouse cerebellar Purkinje cells. *Cell Structure & Function* **16**: 419-432.
- Yamauchi T, Yoshimura Y (1998). Phosphorylation-dependent reversible translocation of Ca2+/calmodulin-dependent protein kinase II to the postsynaptic densities. *Life Sciences* **62**: 1617-1621.
- Yokota S, Atsumi S (1983). Immunoelectron microscopic localization of cathepsin D in lysosomes of rat nerve cells. *Histochemistry* **79**: 345-352.
- Zhang N, Walberg F, Laake JH, Meldrum BS, Ottersen OP (1990). Aspartate-like and glutamate-like immunoreactivities in the inferior olive and climbing system: a light microscopic and semi-quantitative electron microscopic study in rat and baboon (*Papio anubis*). *Neuroscience* **38**: 61-80.

